Physics – Uspekhi **38** (11) 1247 – 1269 (1995)

PACS numbers: 32.90.+a; 42.50.–p

Atomic stabilisation in a laser field

N B Delone, V P Krainov

Contents

Abstract. Physical phenomena arising in the photoionisation of an atom in a laser radiation field are considered. Theoretical studies conducted by means of various methods are reviewed, predicting the existence of the atomic stabilisation effect — the reduction in photoionisation probability with increasing field strength in a fixed radiation field. Various experiments designed to observe the effect are discussed.

1. Introduction

The atomic stabilisation effect denotes the reduction of the atomic photoionisation rate compared with the value given by the Fermi golden rule. The effect is predicted for certain values of laser frequencies and intensities and seems at first to contradict the familiar physical principles of radiation – matter interaction. We should mention those principles here briefly.

For a quantum system in a weak external field of frequency $\omega > E_n/\hbar$, where E_n is the electron binding energy, from the fundamental quantum-mechanical principles the photoionisation rate is

$$w_{nf} = \left(\frac{2\pi}{\hbar}\right)|V_{nf}|^2 \rho_f \qquad (1)$$

N B Delone General Physics Institute, Russian Academy of Sciences
ul. Vavilova 38, 117942 Moscow
Tel. (7-095) 135-02 14. Fax (7-095) 135-02 70
V P Krainov Moscow Institute of Physics and Technology
Institutskii per. 9, 141700 Dolgoprudnyi, Moscow Region
Tel. (7-095) 408-75 90

Received 15 June 1995
Uspekhi Fizicheskikh Nauk **165** (11) 1295–1321 (1995)
Translated by E Strel'chenko; edited by L Dwivedi

(Fermi's golden rule). Here V_{nf} is the matrix element for the transition from a bound state n to a final state f in the continuum spectrum; ρ_f is the density of continuum states. In the case of interest here, with atomic transitions driven by an intense laser radiation field, in the long-wavelength approximation the matrix transition element of the electric dipole is

$$V_{nf} = ez_{nf}F\,,$$

where F is the amplitude of the radiation field (which we specify to be polarised linearly along the Z axis). Then, from Eqn (1)

$$\Gamma_n = w_{nf} \sim F^2 \sim I\,, \qquad (2)$$

where I is the radiation intensity and Γ_n the ionisation width of the initial state n. From Eqn (2) the ionisation lifetime t_n is

$$t_n \sim \frac{1}{w_{nf}} \sim \frac{1}{I}\,. \qquad (3)$$

Until recently, relations (1)–(3) have invariably been found to hold in atomic photoionisation studies and there is no reason to question their validity in a weak external field.

In the mid-1970s, however, a number of theoretical studies were published which predicted different photoionisation processes for field intensities and frequencies above certain critical values. In particular, an ionisation probability w_{nf} inversely proportional to intensity I was predicted. These studies will neither be quoted nor referred to here since, as it is quite clear now, a number of serious objections can be raised on fundamental grounds (see the monograph by the authors, Ref. [1], for the present-day criticism).

In the late 1980s many theorists and a number of experimentalists become preoccupied with the atomic

stabilisa-tion effect. Many well-founded predictions, both classical (for Rydberg states) and (mainly) quantum mechanical, were made all of which carried the same message qualitatively that, starting from certain values of major field and electron parameters (frequency and amplitude; principal quantum number n or the binding energy E_n), some deviations from the Fermi golden rule are expected to develop which must reduce the photoionisation probability and thus produce the 'atomic stabilisation' effect. These theoretical predictions have already been discussed in Refs [1–2] (see also Refs [3–5]) and will be discussed more comprehensively below, with regard for studies as of the autumn of 1995.

Most recently, experiments have been performed which agree to some extent with theoretical predictions. These are also reviewed here. As yet, however, no single experiment has provided a complete and detailed description of the stabilisation effect.

Before the end of this section, a brief discussion of a number of major trend-determining theoretical models seems to be in order. This will enable simple qualitative conclusions concerning the origin of stabilisation to be made.

We start with classical mechanics. Consider a Rydberg state of principal quantum number $n \gg 1$ in which the electron rotates in a highly eccentric Kepler orbit around the atomic core. Let the orbit lie in the XY plane (Fig. 1). As is known, the electron is most likely to absorb a photon in those time intervals where its coupling to the third body, the atomic core, is maximum, that is, when the electron is close to the core. The Coulomb force e^2/r^2 is then comparable with the force eF exerted by the field. The estimate for the relevant distance r is then

$$r = r_0 \sim \left(\frac{e}{F}\right)^{1/2} \tag{4}$$

(throughout this paper, the convention $e = \hbar = m_e = 1$ is used).

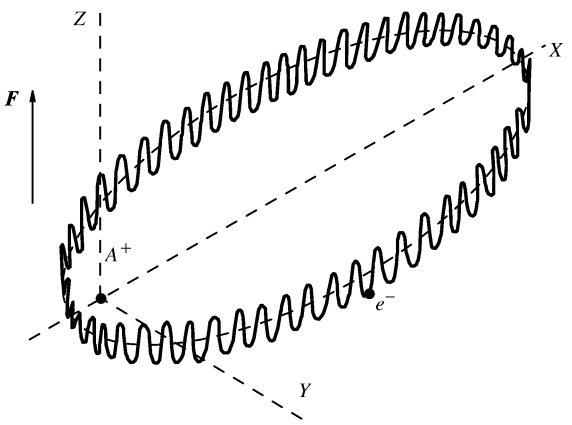

Figure 1. Motion of a Rydberg electron in a highly eccentric state in a high-frequency field linearly polarised along the Z axis.

Now let us place the atom in an external electromagnetic field with vector $\boldsymbol{F}$ normal to the XY plane. We consider the field to be linearly polarised and to have a frequency $\omega > E_n = 1/2n^2$ (photoionisation is allowed). Suppose the amplitude of oscillation of the electron in the field, $a = F/\omega^2$, is sufficiently large ($a \gg r_0$) but at the same time is much less than the Kepler radius $r_n \sim n^2$. These conditions are compatible for $n \gg 1$ since the condition $a \gg r_0$ yields $F \gg \omega^2 (F)^{-1/2}$, i.e.,

$$F \gg \omega^{4/3} \sim \frac{1}{n^{8/3}}\,, \tag{5}$$

whereas from the condition $a \ll r_n$ we have

$$F \ll \omega^2 n^2 \sim \frac{1}{n^2}\,. \tag{6}$$

Under these conditions, the electron follows a complicated trajectory such that its projection on the XY plane corresponds to the original Kepler orbit, while along the Z axis oscillations occur. Then, for certain phase relations between the orbital and electric-field-oriented motions, it is seen from Fig. 1 that when close to the core (at distance r_0) in the XY plane, the electron may be far away from it in the Z direction (at distances of order $a \gg r_0$). Clearly, the probability of photoionisation will in this case be lower than when the electron oscillations are not taken into account [and the probability is determined by Eqn (1)].

As an alternative model, consider an atom in a linearly polarised field, a situation which leads to strong polarisation of the atom. This means that in an external field which is strong enough ($a \gg r_n$, as opposed to the preceding example) the initial wave function of the electron transforms into a qualitatively different spatial distribution, one which has a minimum rather than a maximum near the atomic core, and two distant maxima symmetrical about the core along the field polarisation direction (Fig. 2) (so-called distribution dichotomy). This means that the photoionisation probability must be reduced since the electron spends less time near the core compared with the case when the initial wave-function distribution is assumed unaltered. The critical strength is given by the condition $a \sim r_n$, or

$$F \sim \omega^2 n^2\,. \tag{7}$$

Such stabilisation has come to be known as adiabatic since the new polarised state of the atom evolves adiabatically from its initial unperturbed state. Transitions to other discrete states are of no significance in this process. The concept of an oscillating electron is valid if the radiation frequency ω is large compared with the electron orbital frequency $\omega_n = 1/n^3$ (n is the principal quantum number of the state): Fig. 1 shows that one Kepler period must accommodate many oscillations.

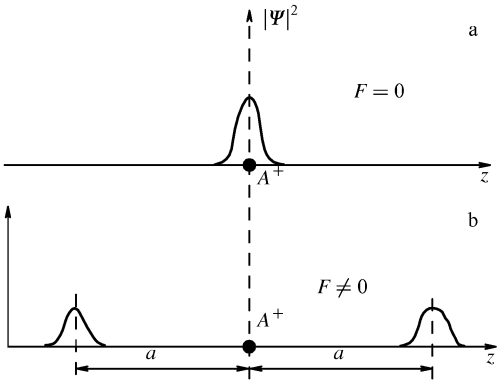

Figure 2. Electron cloud distribution along the direction of a linearly polarised field: (a) $F = 0$; (b) $F \gg \omega^2 n^2$, $a = F/\omega^2$.

Let us consider one more model, a series of Rydberg ($n \gg 1$) states in a high-frequency external field ($\omega > E_n$, where E_n is the energy of the nth state). Clearly, under such circumstances photoionisation from the Rydberg states will occur. For a sufficiently strong field, the ionisation width Γ_n of the initial Rydberg states will reach the order of $\omega_n = \Delta E_{n,n\pm1}$, which is the spacing between these states. The quasicontinuum produced in this way enables three-, five-, and more-photon Raman-type transitions to occur via the continuous spectrum as the atom successively absorbs and emits external-field photons (Fig. 3). For certain assumptions on the matrix elements involved, the interference between different transitions turns out to be destructive (each successive three-, five-, and more-photon matrix element is obtained from its predecessor by multiplying by $i\Gamma_n$, where i is the imaginary unity). This effect reduces the probability of photoionisation from the set of Rydberg states, i.e., leads to the stabilisation of the atom. This is 'interference stabilisation'.

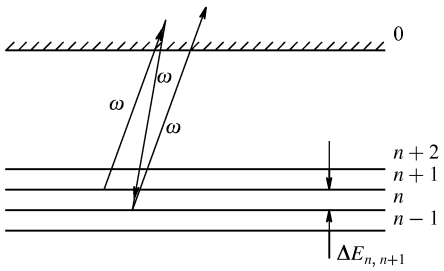

Figure 3. Diagram of Raman transitions between Rydberg atomic states, in third-order perturbation theory.

It is models as simple as those above which provide a basis for rigorous stabilisation predictions. In conclusion, it should be noted that the atomic stabilisation effect is often associated with the superintense strength of the applied field. This does not capture the essence of the problem, however, because the value of the radiation frequency is also important. A more adequate view is that for a given initial state to be stabilised certain critical values of the frequency and strength of the external electromagnetic field must be exceeded.

In what follows, various theoretical approaches predicting the stabilisation effect will be first considered, and then a number of relevant experiments will be analysed.

2. Keldysh – Faisal – Reiss approximation

Within the Keldysh – Faisal – Reiss (KFR) approximation [6 – 8], the amplitude A_{nf} for the transition from an initial field-free atomic state n to a final continuum state f (with a Volkov wave function $\Psi_f^{(V)}$, the core field being neglected) is given by the S matrix element

$$A_{nf} = -i\int_{-\infty}^{\infty} \left\langle \Psi_f^{(V)} \middle| V(\boldsymbol{r},t) \middle| \Psi_n^{(0)} \right\rangle dt \ . \tag{8}$$

Here $\Psi_n^{(0)}$ is the field-unperturbed wave function of the initial bound state of the atom, and $V(\boldsymbol{r},t)$ is the interaction potential between an atomic electron and the electromagnetic field:

$$V(\boldsymbol{r},t) = \frac{\hat{\boldsymbol{p}}\cdot\boldsymbol{A}}{c} + \frac{|\boldsymbol{A}|^2}{2c^2} \ . \tag{9}$$

Here, further, $\hat{\boldsymbol{p}}$ is the electron momentum operator, and $\boldsymbol{A}$ is the field vector potential (specifying the field turn-on and turn-off regimes). The analysis of superintense field ionisation is usually limited to one-electron approximation.

Keldysh [6] limits his treatment to small fields comparable to atomic ones (the atomic field strength is taken to be $F_a = 5.14 \times 10^9$ V cm^{-1}) and to frequencies ω small compared with the atomic binding energy E_n. The ionisation of the atom is then determined by the so-called adiabaticity parameter

$$\gamma = \frac{\omega(2E_n)^{1/2}}{F} \ , \tag{10}$$

where E_n is the unperturbed binding energy of the initial atomic state, and F and ω are the amplitude and frequency of the external field. The field – atom interaction is taken in the 'length gauge' dipole form:

$$V(\boldsymbol{r},t) = \boldsymbol{r}\cdot\boldsymbol{F}\cos(\omega t) \ . \tag{11}$$

If $\gamma \gg 1$, the perturbation theory for the field strength is valid, and ionisation is a multiphoton process according to Keldysh. For the other extreme, $\gamma \ll 1$, ionisation proceeds by tunneling through an effective potential barrier slowly pulsing in time, and the ionisation rate is, to within an exponentially small error, identical to the corresponding result for a static electric field:

$$w_{nf} \sim |A_{nf}|^2 \sim \exp\left[-\frac{2(2E_n)^{3/2}}{3F}\right] \ . \tag{12}$$

For a particle ionised with a short-range potential, the quantity $(2E_n)^{3/2}$ can be called an atomic field strength in accordance with Eqn (12) . However, when it is an atom or a positive ion which is ionised, the preexponential which we omitted in Eqn (12) is important. For highly excited states, this is increasingly so, with the result that the atomic strength approaches the order of $(2E_n)^2$. This approximation is being widely used in describing multiphoton processes in subatomic external fields (see, e.g., Ref. [1]).

However, the general expression (8) applies not only for fields small compared with atomic ones, but also for atomic and superatomic fields. The only requirement for Eqn (8) to hold is that the atomic potential in the final continuum state be negligible. This condition is justified either for a short-range potential, or for high-energy photoelectrons, or for a superintense field, when the atomic potential is relatively unimportant.

Another important point is that expression (8) is nonrelativistic, which sets an upper bound on the strength of the field applied. Relativistic effects become important when the electron velocity in the field, $v_e = F/\omega$, is of the order of the speed of light, $c = 137$ a.u. For the range of frequency of light this means that relativity shows up at radiation intensities above 10^{18} W cm^{-2}, and for the CO_2 laser even above 10^{16} W cm^{-2}; these values are already well within the reach of very powerful lasers.

The nonrelativistic nature of electron motion provides the justification for the dipole approximation, in which the vector potential $\boldsymbol{A}$ in Eqn (9) (as well as the radiation electric field) depends only on the time t and not on the combination $t - \boldsymbol{k}\cdot\boldsymbol{r}/\omega$ ($\boldsymbol{k}$ is the wave vector of the electromagnetic wave). This, of course, does not rule out the dependence of $\boldsymbol{A}$ on coordinates related to the laser focusing problem.

From Eqns (8) and (9), for the simple case of ground-state hydrogen ionised by the abrupt turn-on of a circularly polarised electromagnetic field, we obtain the following expression for the ionisation rate $dw/d\Omega$ to the solid angle element $d\Omega$ [8]:

$$\frac{dw}{d\Omega} = \frac{4}{\pi(2\omega)^{3/2}} \times \sum_{N=N_0}^{\infty} \frac{(N - z - 1/2\omega)^{1/2}}{(N-z)^2} J_N^2 (z^{1/2}K) . \quad (13)$$

Here N is the number of the photons absorbed,

$$N_0 = \left\{ \frac{1}{2\omega} + z \right\} \quad (14)$$

is the minimal number of absorbed photons, $\{\ldots\}$ is the integer part of a number,

$$z = \frac{F^2}{2\omega^3} \quad (15)$$

is the dimensionless field strength parameter, and

$$K = 2\left(N - z - \frac{1}{2\omega}\right)^{1/2} \sin\theta , \quad (16)$$

where θ is the angle between the direction of the ejected photoelectron and that of the circularly polarised radiation. Expression (13) does not require the photon frequency ω to be small compared with the ionisation potential of hydrogen.

Note that expression (14) takes account of the AC-Stark shift in the field of the circularly polarised wave. The shift determines the edge of the continuum and is equal to $F^2/2\omega^2$.

From Eqn (15) it is seen that the lower the field frequency ω the lower the value of field strength F required to achieve high values of the dimensionless intensity parameter z.

Mathematically, the boundedness of the probability $dw/d\Omega$ in Eqn (13) is due to the boundedness of the Bessel functions. In Fig. 4 replotted from Ref. [9], the ionisation rate integrated over the electron escape angles is shown plotted against the laser intensity $I = cF^2/4\pi$ for two frequencies, $\omega = 1/128$ a.u. and $\omega = 2$ a.u., respectively, which are small and large compared with the hydrogen ionisation potential. From Fig. 4 stabilisation over a wide range of field frequencies is evident. Also, the lower the frequency the smaller the value of the critical field, this latter marking the crossover from the increasing to the decreasing ionisation probability. The explanation is that the ionisation rate given by Eqn (13) is determined by the dimensionless parameter z [Eqn (15)] which increases as ω decreases. In particular, at $\omega = 1/128$ a.u., the critical intensity is of the order of 10^{15} W cm^{-2}, i.e., small compared with the atomic intensity.

In the low-frequency ($\omega \ll 1$) weak-field case (see below), Eqn (13) is shown to agree with the original Keldysh theory, the nature of ionisation (i. e., tunneling- or multiphoton-type) depending on the adiabaticity parameter given by Eqn (10). Weak fields in Eqn (13) correspond to the Bessel functions having arguments close to their indices, when for $\omega \ll 1$ we have $N \gg 1$, and depending on $\gamma \lesseqgtr 1$ the Debye asymptotic expansion for the Bessel functions may lead to either an (tunneling) exponential or a (multiphoton) power-law dependence.

As already noted, this approximation has a significant disadvantage of neglecting the atomic potential in the final continuum Volkov state. Ref. [10] remedies this for ground-state hydrogen ionisation with circular polarisation provided $F/\omega^2 \gg 1$ [see Eqn (7) for $n \sim 1$], when the amplitude of classical electron oscillations in the electromagnetic wave field is much larger than the Bohr radius. Note that this is a rather mild condition for a low-frequency field.

The dependence of the ionisation rate on the intensity I is shown in Fig. 5 for $\omega = 0.043$ a.u. (wavelength $\lambda = 1.06$ μm). It is seen that including the Coulomb potential in the final state increases the ionisation rate by several orders of magnitude at subatomic fields but is of no significance in the stabilisation region (in this case, for $I > 10^{-1}$ a.u.).

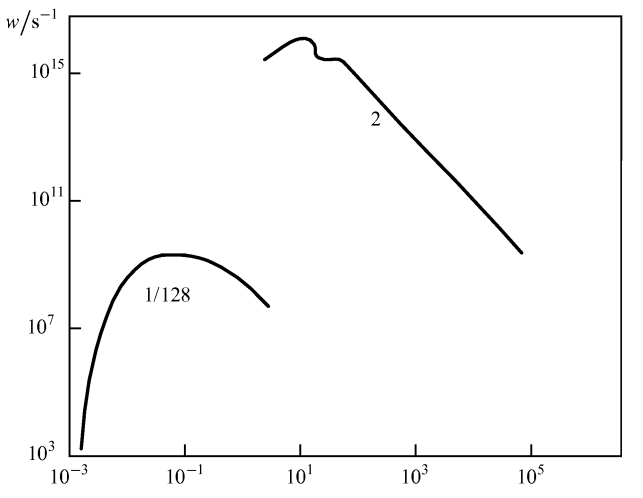

Figure 4. Ionisation rate of ground-state hydrogen against radiation intensity for $\omega = 1/128$ a.u. and $\omega = 2$ a.u. (circular polarisation) [9].

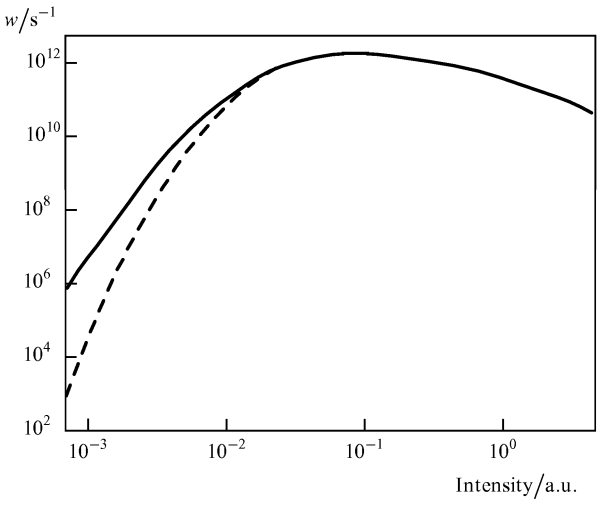

Figure 5. Ionisation rate of ground-state hydrogen against radiation intensity for $\omega = 0.043$ a.u. (circular polarisation) [10]. The dashed line gives the final-state wave function and the solid line gives the same function with the Coulomb potential included in the final continuum state.

The results depend essentially on the way the Volkov wave functions are treated. For example, instead of the S matrix approach of Eqn (8), it has been suggested [11] that the Volkov packet be constructed as a linear combination of wave functions of the form

$$\Psi(\boldsymbol{r},t)=\int \Psi_n^{(0)}(\boldsymbol{p})\,\Psi_p^{(V)*}(\boldsymbol{r},t)\,\mathrm{d}\boldsymbol{p}\ . \tag{17}$$

Here $\Psi_n^{(0)}(\boldsymbol{p})$ is the Fourier component of the unperturbed atomic wave function (the case considered was again ground-state hydrogen). For $t=0$ Eqn (17) yields

$$\Psi(\boldsymbol{r},0)=\Psi_n^{(0)}(\boldsymbol{r})\ , \tag{18}$$

showing that the electron was in the (hydrogen) ground state initially.

The absolute probability for the atom to remain in its initial state by the time t is determined by the overlap of the wave functions (17) and (18), i.e.,

$$W(t)=\left|\left\langle \Psi_n^{(0)}\boldsymbol{r}\right)\left|\Psi(\boldsymbol{r},t)\right\rangle\right|^2\ . \tag{19}$$

In Fig. 6 the quantity $W(t)$ calculated for $\omega=1.5$ a.u. and $F=5$ a.u. is shown as a function of time (the time being measured in field cycles [12]). Again circular polarisation is considered. The atom is seen to ionise fully within a fraction of a cycle and hence no stabilisation occurs.

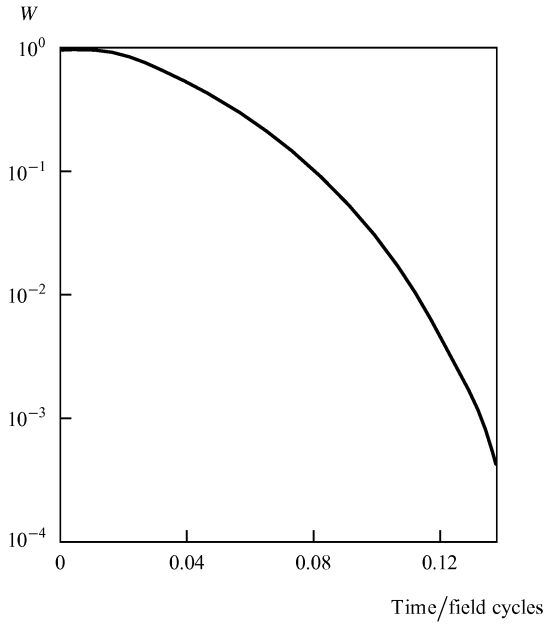

Figure 6. The absolute probability for a hydrogen atom to remain in the ground state by a given time in a circularly polarised field with a frequency $\omega=1.5$ a.u. and amplitude $F=5$ a.u. [12].

The conclusion we are led to is that in considering the problem of stabilisation it is essential to know which quantity is being evaluated and precisely how the Volkov approximation for the final state is being used. In particular, Eqn (17) implies that, if the electron has acquired the momentum $\boldsymbol{p}$, its subsequent evolution in time is that of a free electron in an external electromagnetic field. The same follows from the S matrix expression (8). However, different mathematical realisations of this physical model have produced opposite results for the case of a superintense field because of the uncertainty as to when this approximation is valid.

This conclusion is also supported by an S matrix analysis with the electron–core potential $U(r)$ replacing Eqn (9). For the transition amplitude we then have, instead of Eqn (8),

$$A_{nf}=-\mathrm{i}\int_{-\infty}^{\infty}\left\langle \Psi_n^{(0)}\right|U(r)\left|\Psi_f^{(V)}\right\rangle \mathrm{d}t\ . \tag{20}$$

For a superatomic field ($F\gg F_\mathrm{a}$) this yields a simple dependence [13]

$$w\sim|A_{nf}|^2\sim\frac{F_\mathrm{a}}{F}\ , \tag{21}$$

where from Eqn (8) we find [14]

$$w\sim\left(\frac{F_\mathrm{a}}{F}\right)^2\ . \tag{22}$$

As noted, in Keldysh's original work [6] instead of Eqn (9) the nonrelativistic-dipole 'length-gauge' perturbation [Eqn (11)] was used. Then in the case of a super-intense field, the ionisation rate increases monotonically with F with no stabilisation being exhibited [14]. It should be emphasised, however, that it is expression (9) which follows from the general relativistic S matrix expression in the nonrelativistic limit [9]. While first-order perturbation predictions are identical, differences appear from the second order on. In this sense, expression (9) should be preferred to expression (11), although for two- and three-level systems interacting with an electromagnetic field the reverse situation occurs [15].

All in all, the conclusion to be drawn from the above is that the KFR S matrix approximation supports rather than opposes stabilisation in a superintense field. The results above show, however, that the picture is as yet not completely clear and further calculations are required, as is an analysis of whether the atomic core potential may be neglected in the final continuum state.

The remark which follows relates to the dependence of stabilisation on the polarisation of the radiation. For the ground-state hydrogen atom it has been shown [16] that in a circularly polarised field the ionisation rate first monotonically increases with the field strength and then monotonically decreases when the field becomes superintense. With linear polarisation, however, the field dependence of the ionisation rate is nonmonotonic and displays a large number of local maxima and minima. Moreover, at the same field strength circular polarisation stabilises the ground-state hydrogen atom much more effectively than linear polarisation. An explanation is that, in the latter case, much of a field cycle corresponds to relatively low (in particular, atomic) strengths: at these times the ionisation probability is much greater than at times when the field strength reaches its peak value. A similar sharp nonmonotonicity in the case of linear polarisation is predicted for the three-dimensional zero-range potential [17].

Within the KFR framework, not only the ionisation probability but also the energy and angular distribution of the ejected electrons can be calculated. The energy spectrum is found from the basic formula (8) by fixing the energy of the final continuum state f and studying how the ionisation rate depends on this energy at a specified field strength. Eqn (13) corresponds to analysing individual terms in the

sum over N absorbed photons. The dependence of the ionisation rate on the angle θ is determined by the parameter given by Eqn (16).

With the experimental check in mind, it should be remembered that the ionisation probability tends to saturate during a pulse. For the case of radiation with a realistic Gaussian intensity distribution in space and time, this effect was taken care of in Ref. [18]. The results were compared with the experimental spectra of Ref. [19] for helium atoms subjected to 815 nm circular and 820 nm linear laser radiation. The peak intensity was $I = 1.275 \times 10^{15}$ W cm^{-2} (circular polarisation) and $I = 3.15 \times 10^{15}$ W cm^{-2} (linear polarisation)—both corresponding to the above-barrier decay. The electron oscillation amplitude, for example, for circular polarisation, was found to be $a = F/\omega^2 = 43$ a.u., much greater than the size of the helium atom, so that the field can be considered as superintense [see condition (7)].

In Fig. 7, as an example, the experimental spectra of Ref. [19] and those calculated based on Ref. [10] are shown for the case of circular polarisation; the agreement is seen to be good. In the calculations, the Hartree–Fock approximation was used for the ground state of helium.

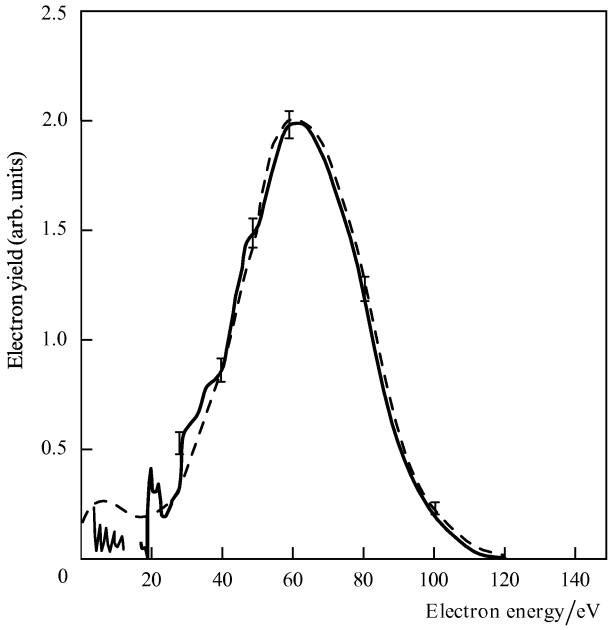

Figure 7. Electron energy spectra for the case of circular polarisation. Solid line—experimental data of Ref. [19]; dashed line—theoretical calculation [18]. Ionisation of the helium atom by a $\lambda = 815$ nm laser pulse with peak intensity $I = 1.275 \times 10^{15}$ W cm^{-2}.

It is seen that the peak of the distribution occurs when the energy of the electron is equal to its oscillatory energy $F^2/2\omega^2 = 60$ eV in a circularly polarised field—this is consistent with theoretical predictions. The same is true for subatomic fields (see Ref. [1], Section 4.3.2).

Similar linear polarisation results are shown in Fig. 8. Here the average oscillatory energy of the electron is $F^2/4\omega^2 = 150$ eV. Theory and experiment agree well, with the peak of the distribution occurring at zero energy. The theoretical dependence is obtained in Ref. [18] on the basis of the S matrix approach of Ref. [8].

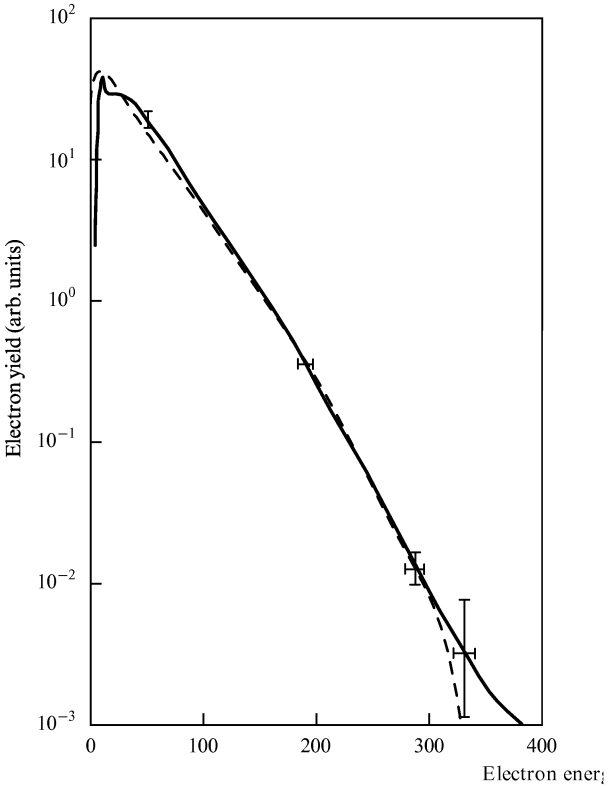

Figure 8. Electron energy spectra from helium in a linearly polarised field with wavelength $\lambda = 820$ nm and peak intensity $I = 3.15 \times 10^{15}$ W cm^{-2}. Solid line—experimental data of Ref. [19]; dashed line—theoretical calculation [18].

As for the short-range three-dimensional potential, it has been shown [9] that, in the S matrix approximation [Eqn (8)] the ionisation probability for a single bound state supported by the zero-range potential decreases monotonically with the field—that is, no stabilisation occurs.

The same result is obtained by exact calculation for a particle ionised from a zero-range potential perturbed by a superintense circularly polarised field [20]. The treatment involves the solution of the exact integral equation obtained from the stationary Schrodinger equation in the reference frame rotating with frequency ω relative to the laboratory frame [21] (see the next section for more details).

However, numerical calculations for short-range potentials do predict stabilisation in certain intensity ranges (see Section 3).

In summary, if one uses the S matrix approximation or invokes related schemes which also, in one way or another, take account of the Volkov wave functions for the final continuum state of the electron, it is found that the superintense field ionisation problem is very sensitive to the detailed nature of the particular method employed. While most calculations do favour the stabilisation effect, the validity of the S matrix approximation for atoms is in some doubt [12].

3. Numerical work

The numerical solution of the Schrodinger equation makes it possible to obtain ionisation probability in superintense fields. Such solutions are free from shortcomings which the S matrix method (outlined in the preceding section) and

other approximate methods (see the following section) possess. However, numerical solutions can be carried out only for particular fixed values of the relevant parameters (radiation field strength F and frequency ω, the binding energy E_n of the unperturbed atomic state, etc.), and in particular they cannot be extended to the $F \to \infty$ case.

Thus, we consider here various numerical solutions of the time-dependent Schrodinger equation

$$i\frac{\partial \Psi}{\partial t} = \left[-\left(\frac{\Delta}{2}\right) + U(r) + V(\boldsymbol{r},t)\right]\Psi(\boldsymbol{r},t) \ . \tag{23}$$

Here $U(r)$ is the electron–core potential, and $V(\boldsymbol{r},t)$ is the electron–field interaction, given by Eqn (9) or Eqn (11). The initial condition of the Cauchy problem is of the form

$$\Psi(\boldsymbol{r},-\infty) = \Psi_n^{(0)}(\boldsymbol{r}) \ ,$$

where $\Psi_n^{(0)}(\boldsymbol{r})$ is the unperturbed initial-state wave function. This formulation is in line with the experimental situation, in which laser radiation with a specified pulse envelope acts on an isolated atom, the ionisation probability per pulse of which is calculated. The problem is difficult computationally, however, since even for the one-electron case the wave functions depend on four independent variables $\boldsymbol{r},t$.

In a computationally simpler formulation, the eigenvalue solution to Eqn (23) is found by expanding $\Psi(\boldsymbol{r},t)$ on some complete basis of the unperturbed states and then diagonalising the high-rank matrix which results (the rank being equal to the number of states taken). The diagonalisation process enables the complex energies of the perturbed states to be found. The real part of the energies determines the Stark shift of the levels, and the imaginary gives the ionisation rate of the state. The classification of the perturbed states envisages an adiabatic turn-off of the field, the states in question being transformed into the corresponding unperturbed states in this process. The following example illustrates this approach.

One of the first problems to be addressed was the ionisation of ground-state hydrogen by a superintense field. The problem is solved numerically in Ref. [22] as an eigenvalue problem. The solution to Eqn (23) is presented in the form

$$\Psi(\boldsymbol{r},t) = \exp(-iEt)f(\boldsymbol{r},t) \ , \tag{24}$$

where the function $f(\boldsymbol{r},t)$ is periodic in time, with the same period as the external electromagnetic field. Equation (24) is a consequence of the Floquet theorem for temporal periodic perturbations (see, e.g., Ref. [15] for more details). This implies that the field strength amplitude is constant.

Next the periodic function $f(\boldsymbol{r},t)$ is Fourier transformed with respect to time, and the resulting coefficients, which are functions of the coordinate $\boldsymbol{r}$, are expanded on the basis of Sturmian functions for the Coulomb problem. The advantage of the Sturmian over the unperturbed Coulomb basis set is that, in the former, all functions belong to a discrete spectrum and are therefore computationally convenient from the point of view of convergence of the series as the number of its terms is increased.

Further, the radial coordinate $\boldsymbol{r}$ must be replaced by $r \to r\exp(i\alpha)$, where α is a certain angle between 0 and $\pi/2$ (see Ref. [23]), in order to avoid Sturmian-related divergences (an alternative approach has been proposed for the above-threshold ionisation problem in hydrogen [24]). This procedure is called the 'complex rotation of the coordinate.'

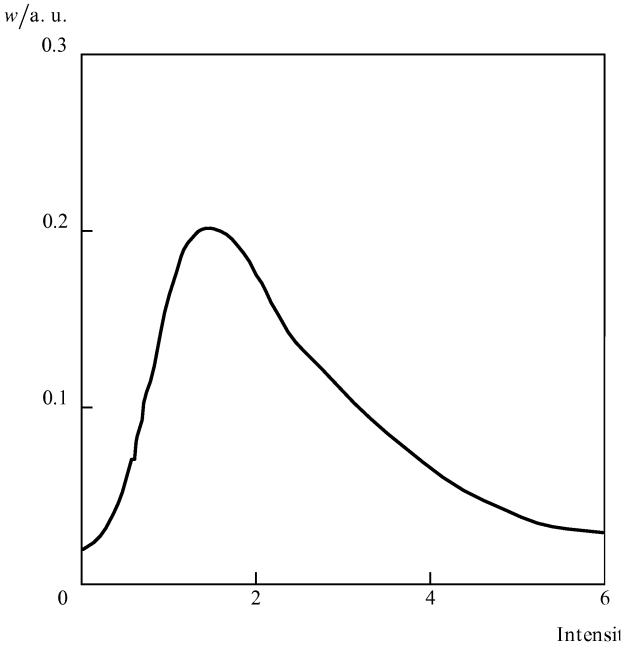

Figure 9. Ionisation rate of ground-state hydrogen as a function of intensity for the case of linear polarisation with $\omega = 0.65$ a.u. [22].

By truncating the basis beyond a certain number N and verifying that results remain unchanged as the basis size is increased, we can equate the determinant of the $N \times N$ matrix to zero (i.e., diagonalise the Hamiltonian) and thus find the complex value of the Floquet energy in expression (24). It is the imaginary part which determines the ionisation rate.

The numerical analysis of Ref. [22] was performed for a field frequency of 0.65 a.u., which exceeds the hydrogen ionisation potential. The intensity (I) dependence of the ionisation rate w for linear polarisation is shown in Fig. 9. The peak probability occurs at $I = 1.1 \times 10^{16}$ W cm^{-2}. After the peak, w decreases monotonically with I, which in effect is the stabilisation of ground-state hydrogen in the superintense field. Since the electron takes time $t_n = 2\pi n^3 = 2\pi$ a.u. to orbit around the proton at $n = 1$, at the maximum point $wt_n = 1.2$, which shows that the atom ionises within about a single revolution of the electron.

Thus, the results of Ref. [22] confirm the effect of the ground-state stabilisation of hydrogen in a high-frequency superintense field. Some doubt may arise if one considers that the stronger the field, the larger the basis required to diagonalise the Hamiltonian numerically; this point was not verified in the numerical procedure because of the dramatic increase in the computation time required.

A problem of greater computational complexity, the ionisation of three-dimensional ground-state hydrogen by a superintense pulse, is addressed in Ref. [25]. The approach used is to solve the Cauchy problem and to evaluate the total ionisation probability W during the laser pulse. The field frequency is taken to be $\omega = 1$ a.u., twice the atomic ionisation potential, and the pulse length varied from 1 to 12 field cycles. Although above 10^{16} W cm^{-2}, W decreased somewhat with increasing intensity, it remained greater than unity. It is this decrease which is termed the stabilisation effect.

Thus, the effect does not depend on the particular numerical method used. Numerical solutions indicate the

existence of the stabilisation effect. Analysis of the total probability $W(t)$ shows that it is proportional to time t only for fields smaller than atomic ones and for not very large values of t, when no saturation occurs. For atomic and superatomic fields, the linear $W(t)$ regime is virtually absent, the concept of ionisation rate is meaningless, and the variation of $W(t)$ with time t is oscillatory.

The three-dimensional Coulomb potential was not the only one used in the numerical work on quantum systems in superintense fields. In Refs [26–27] the two-electron one-dimensional ion H^- with a core potential of the form $(1+x^2)^{-1/2}$ (which goes over to the Coulomb potential at large distances) was considered. The Cauchy problem for the one-dimensional time-dependent Schrodinger equation was solved and the total ionisation probability for the time t calculated. It is concluded that the electron–electron interaction does not reduce the tendency of the ion to stabilise as the laser field increases.

In Ref. [20], which we referred to earlier, the ionisation rate w was calculated for a three-dimensional zero-range potential perturbed by a superintense circularly polarised field. In the reference frame rotating with the electric field vector of the wave, the Schrodinger equation is stationary and reduces to a simple integral equation for the complex energy [21]. The imaginary part of this energy determines the ionisation rate and, for $F \gg F_a = (2E_0)^{3/2}$, takes the simple form

$$w = 0.303\, F^{2/3} \ . \tag{25}$$

The unperturbed energy of the (single) bound state was taken to be $E_0 = -1/2$, and $m = \hbar = 1$. Thus, stabilisation is absent in this case. A similar conclusion has been reached for linear polarisation [28], although no analytical expressions of the type given by Eqn (25) exist in this case.

In Ref. [29] a one-dimensional square-well potential of finite radius and depth carrying a single bound state is solved. The external field is taken to be linearly polarised. The Schrodinger equation (23) is solved by direct numerical integration, and the total ionisation probability is calculated. It is shown that in superintense fields the probability decreases with the field, that is, the stabilisation of the bound state takes place. The energy of the state is equal to the oscillatory energy $F^2/4\omega^2$, which in this case greatly exceeds the unperturbed binding energy of the particle in the potential well. Thus, there is a difference between the zero-range and short-range results for finite-width finite-depth potentials.

The general conclusion from the numerical work is that the stabilisation of a quantum system increases as the atomic potential becomes less singular. We shall see later that classical mechanics confirms this conclusion.

4. The Kramers–Henneberger approximation

Despite the existence of other effective approximations, the method of Kramers and Henneberger [30] is currently being used to analyse the dynamics of quantum systems in superintense monochromatic fields.

The method involves changing to a noninertial frame of reference in which the electron in an electromagnetic wave field is at rest. Taking a linearly polarised field as an example (although it is the circular field to which the method was actually applied), this implies changing to the so-called Kramers frame co-oscillating with the electron. The electron coordinate in this frame, $\boldsymbol{r}'$, and that in the laboratory frame, $\boldsymbol{r}$, are then obviously related by

$$\boldsymbol{r}' = \boldsymbol{r} - \left(\frac{\boldsymbol{F}}{\omega^2}\right)\cos\omega t \ . \tag{26}$$

Here again $\boldsymbol{F}$ and ω are the amplitude strength and frequency of the (linearly polarised) field. The transition to this system from the Schrodinger equation (23) is achieved by means of the time-dependent unitary transformation

$$\Psi_{KH}(\boldsymbol{r}', t) = \exp\left[\mathrm{i}\int_{-\infty}^{t} V(\boldsymbol{r}, t)\,\mathrm{d}t\right]\Psi(\boldsymbol{r}, t) \ . \tag{27}$$

In the dipole approximation, the electron–field interaction $V(\boldsymbol{r}, t)$ may be written either in the form of Eqn (9) or — more conveniently in the present context — in the form of Eqn (11).

Substituting Eqn (27) into Eqn (23) gives the following equation for the wave function $\Psi_{KH}(\boldsymbol{r}', t)$ in the oscillating Kramers frame:

$$\mathrm{i}\frac{\partial\Psi_{KH}(\boldsymbol{r}', t)}{\partial t} = \left\{-\frac{\Delta'}{2} + U\left[\boldsymbol{r}' + \frac{\boldsymbol{F}}{\omega^2}\cos(\omega t)\right]\right\}\Psi_{KH}(\boldsymbol{r}', t) \ , \tag{28}$$

where U is the atomic potential and Δ' the Laplace operator with respect to $\boldsymbol{r}'$. By means of a Fourier transform of the periodic potential U over time we find the expression

$$U\left[\boldsymbol{r}' + \frac{\boldsymbol{F}}{\omega^2}\cos(\omega t)\right] = \sum_{N=-\infty}^{\infty} U_n(\boldsymbol{r}')\exp(\mathrm{i}N\omega t) \ , \tag{29}$$

where the Fourier component is defined by

$$U_N(\boldsymbol{r}') = \frac{1}{2\pi}\int_0^{2\pi} U\left[\boldsymbol{r}' + \frac{\boldsymbol{F}}{\omega^2}\cos(\omega t)\right] \times \exp(-\mathrm{i}N\omega t)\,\mathrm{d}(\omega t) \ . \tag{30}$$

The proper Kramers–Henneberger (KH) approximation is obtained, in its simplest from, by neglecting in Eqn (29) all the modes except the mode $N = 0$. The problem then reduces to the solution of the stationary Schrodinger equation for the KH potential [30]:

$$\mathrm{i}\frac{\partial\Psi_{KH}}{\partial t} = \left[-\frac{\Delta'}{2} + U_0(\boldsymbol{r}')\right]\Psi_{KH}(\boldsymbol{r}', t) \ . \tag{31}$$

The remaining $N \neq 0$ harmonics may be neglected in the high-frequency limit [Eqn (31)] provided

$$\omega \gg E_{KH} \ , \tag{32}$$

where E_{KH} is the ground-state energy in the KH potential

$$U_0(\boldsymbol{r}') = \frac{1}{2\pi}\int_0^{2\pi} U\left[\boldsymbol{r}' + \frac{\boldsymbol{F}}{\omega^2}\cos(\omega t)\right]\mathrm{d}(\omega t) \ . \tag{33}$$

As will be seen later, the quantity E_{KH} always tends to zero (but remains negative) as the (superintense) field strength is increased. Consequently, at a given field strength the value of F may be rather small according to Eqn (32) — much lower, in particular, than the binding energy of the unperturbed ground state. This actually implies that for any, even small, ω value one can always find a superintense field value F_c beyond which the inequality (32) will hold and the KH approximation will be valid.

At superintense values of intensities the KH potential [Eqn (33)], in contrast to the atomic $U(r)$, always has a

characteristic two-well form (for a linearly polarised field). The distance from each well to the centre of the potential is equal to the amplitude $a = F/\omega^2$ of the oscillatory motion of the free electron in the electromagnetic wave field. Moreover, the number of states in the KH potential increases with increasing intensity. The new bound states come from the continuum, move some distance into the discrete spectrum, and then approach the edge of the continuum as the intensity increases [32]. Also the energies of all the states that already exist in the atomic potential $U(r)$ tend to zero as the intensity increases. Note that all the energies are calculated in the oscillating Kramers frame. If we change to the laboratory frame, to each energy $F^2/4\omega^2$ should be added the oscillatory energy of the electron (for a linearly polarised field).

As an example, Fig. 10 shows how the hydrogen ground-state energy in the KH potential [Eqn (33)] depends on the amplitude $a = F/\omega^2$ of the back-and-forth motion of the electron in a linearly polarised field [32].

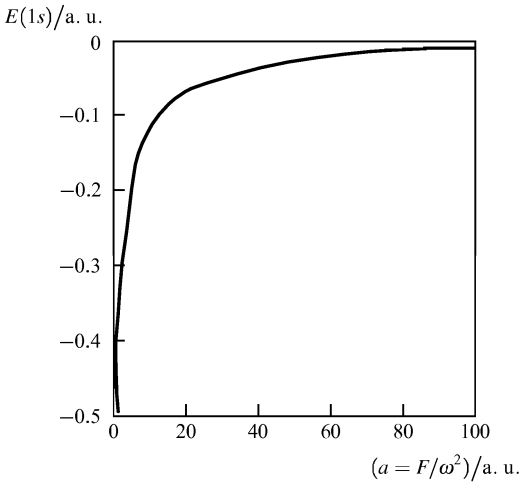

Figure 10. Ground-state energy of hydrogen against the electron oscillatory amplitude in a linearly polarised field [32].

A similar picture is obtained for circular polarisation. In particular, for a superintense field, i.e., under the condition $a = F/\omega^2 \gg 1$, Ref. [33] presents an analytical expression for ground-state hydrogen in the KH potential given by Eqn (33):

$$E_{\mathrm{KH}} = -\frac{\ln a + 2.65}{2\pi a} . \tag{34}$$

As for the KH ionisation of a superintense field, both the rate and the total probability over a given time interval have been calculated. The low-N nonzero Fourier components given by Eqn (30) were included in the calculations. In Fig. 11, the ionisation rate of ground-state hydrogen for a linearly polarised field is plotted against the field intensity for $\omega = 4$ and $\omega = 0.25$ a.u. [32]. Stabilisation is seen at both values, even though at $\omega = 0.25$ a.u. the photon energy is lower than half the ionisation potential. Note, however, that for the stabilisation effect to occur, the less severe condition (32), satisfied for the parameter ranges indicated in Fig. 11, is sufficient. At lower intensities condition (32) does not hold, and therefore at $\omega = 0.25$ a.u. the curve in Fig. 11 is truncated to the left of intensity $I = 1$ a.u., i.e., the maximum of the curve is not shown.

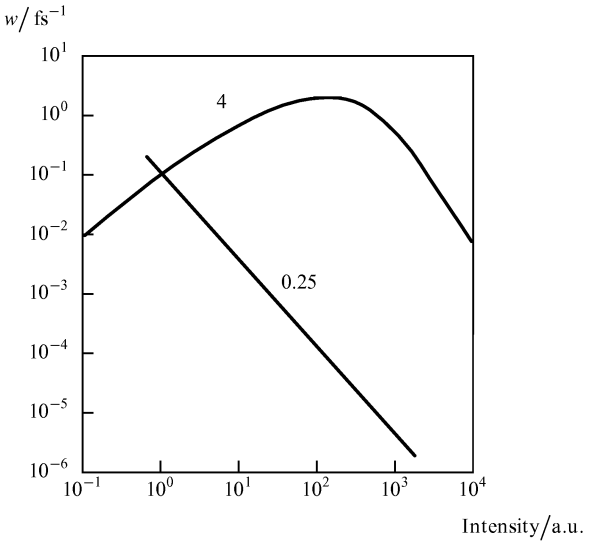

Figure 11. Ionisation rate of ground-state hydrogen against the intensity of a linearly polarised field with $\omega = 0.25$ a.u. and $\omega = 4$ a.u. The calculations are taken from Ref. [32].

We see that the atomic field, defined here as that corresponding to the maximum ionisation probability, increases with frequency. A similar picture emerges from the Keldysh–Faisal–Reiss approximation (see Section 2).

As for the total ionisation probability over the pulse, KH calculations for a one-dimensional Coulomb potential smoothed close to the origin of the coordinates have been performed [34]. The pulse envelope was taken in the form $\sin^2(t/t_l)$, where t_l is the length of the pulse. The effect of stabilisation here manifests itself in that the ionisation probability over the pulse decreases with increasing field strength F. For example, when $\omega = 14.13$ eV the total ionisation probability is unity for $F = 1$ a.u. and 0.5 for $F = 5$ a.u. It should be noted, however, that the value 0.5 is reached in the first field cycle, so that it is unclear whether it is adequate to average the KH potential over a cycle—which is precisely what is done in our approximation because Eqn (30) gives us expression (33).

The stabilisation effect within the KH approximations was also obtained in other calculations [29, 35–37].

As the intensity increases, so does the number of harmonics [Eqn (30)] to be retained in the Schrodinger equation (29) in the Kramers approach [29]. If these are very many, however, the method has no advantage over the direct numerical solution of the Schrodinger equation (whether in the Kramers frame or the laboratory frame). Consequently, alternative approaches to the solution of the Schrodinger equation in the Kramers frame have been developed. One of these is to expand the solution of Eqn (28) in terms of the Floquet states (see Section 3) in the Kramers frame [38–39]. It is found that, for a field frequency lower than the ionisation potential, the ionisation rate for the hydrogen ground state has only a local maximum (a 'window of stability') and that at very high intensities it rises again. In Fig. 12, the dependence of the ionisation rate w on intensity I for $\lambda = 117$ nm radiation is illustrated.

Note here that there is a certain relationship between the present and the previous solution methods: Eqn (31) corresponds to the zeroth Floquet component in the wave function. However, in the Floquet method, as applied to the

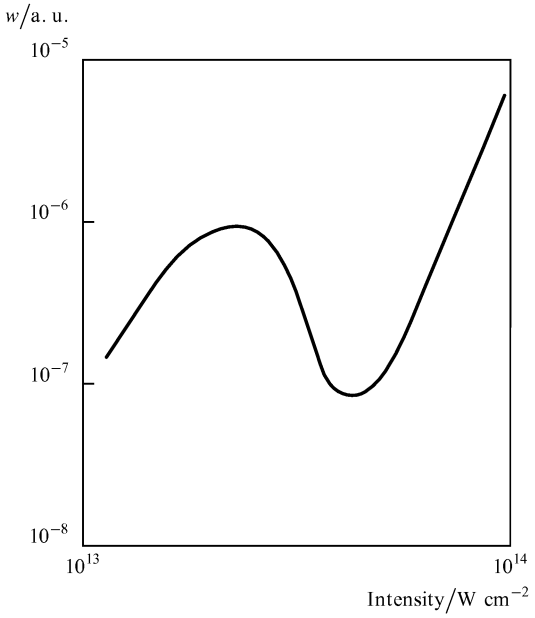

Figure 12. Ionisation rate of ground-state hydrogen against the intensity for the wavelength $\lambda = 117$ nm. The calculations are taken from Ref. [38].

present problem, it turns out that all the components are interrelated through a (formally infinite) system of coupled linear differential equations with respect to the radial coordinate r'.

Restricting numerical calculations to a sufficiently large but finite number of Floquet states and setting the determinant of the system to zero, we obtain an equation for complex Floquet quasi-energies. Their real part determines the Stark shift of the level, and the imaginary part the ionisation rate. This also shows the disadvantage of using the Floquet method for solving the Schrodinger equation: although it yields the ionisation rate, the method does not allow us to calculate the total ionisation probability over the pulse, nor the energy and angular distributions of the photoelectrons ejected.

Thus, depending on the specific KH technique used, different results, namely, atomic stabilisation or a 'stabilisation window' will emerge. The questions that arise in the low-frequency case are particularly numerous. First, one cannot be fully confident of Eqn (32) as a criterion for the KH approximation. In Ref. [40], for example, this criterion was checked against the exactly solvable case of a one-dimensional harmonic oscillator in a linearly polarised field (in the dipole approximation). The exact solution for the quasienergy in this case is

$$E_n = \left(n + \frac{1}{2}\right)\omega_0 + \frac{F^2}{4(\omega^2 - \omega_0^2)}\,, \tag{35}$$

where n represents the oscillatory level (quantum number), ω_0 is the oscillator frequency, and ω and F are the the field frequency and strength amplitude, respectively.

Alternatively, in the KH approximation

$$E_n = \left(n + \frac{1}{2}\right)\omega_0 + \left(\frac{F^2}{4\omega^2}\right)\left(1 + \frac{\omega_0^2}{\omega^2}\right)\,. \tag{36}$$

Comparing Eqns (35) and (36), we find that the KH applicability criterion is $\omega \gg \omega_0$, which disagrees with Eqn (32). A possible reason for this is the absence of a continuous spectrum in the harmonic oscillator problem. However, as criterion (32) is a postulate rather than a proven result, the conclusion that the picture is not yet completely understood is the only one to be content with here.

Furthermore, the stabilisation effect may also be very sensitive to whether it is a one-, two-, or three-dimensional atom to which the KH approximation is applied. It has been shown, for example, that in one dimension the effect is much stronger than in two dimensions [41].

So far we have considered the application of the KH approximation to the ground states of quantum systems. We turn next to Rydberg atomic states. In Ref. [42] the ionisation of circular hydrogen Rydberg orbits ($n \gg 1$, and $m = l = n - 1$) by a superintense field of linear polarisation was studied. The state considered was $n = 7$, $l = m = 6$. The energy of the photon of the external electromagnetic field was taken to be $\hbar\omega = 1.17$ eV, i.e., much greater than the ionisation potential of the state under study, $E_n = 1/2n^2$. Thus condition (32) for the applicability of the KH approximation is fulfilled over the entire range of field strengths. Under these conditions, the ionisation of the KH state [i.e., of the state given by the solution of Eqn (31) which goes over to the required Rydberg state as the field is turned off adiabatically] is of the one-photon type, i.e., in Eqn (30) the $N = 1$ term is the one which dominates the ionisation probability.

The intensity dependence of the ionisation probability for a given Rydberg state is fully analogous to the curve in Fig. 11 for the high-frequency ($\omega = 4$ a.u.) ionisation of ground-state hydrogen. For the case $\omega = 1.17$ eV mentioned above, the peak probability occurs at $I_c = 7 \times 10^{13}$ W cm^{-2}, which may be called a critical value in this example. To this intensity there corresponds $E_c = 0.044$ a.u. Note that the estimate given by Eqn (7) in the Introduction, based on equating the electron oscillation amplitude to the Bohr radius of a given Kepler orbit, yields $E_c = 0.092$ a.u. If we consider that this estimate is valid to within a numerical factor of order unity, the two values of E_c agree quite well. Also, from calculations of Ref. [42], the position of the peak intensity, i.e., the value of I_c, increases with the principal quantum number n of the Rydberg state, the field frequency ω being fixed. This also agrees with the estimate given by Eqn (7).

Thus the critical strength estimate [Eqn (7)] in the KH approximation is adequate in that it reflects the onset of dichotomy at $F > F_c$ (see the Introduction), precisely the point at which atomic stretching along the field polarisation axis starts to occur.

As a matter of fact, it is only at such fields, i.e., if

$$a = \frac{F}{\omega^2} > n^2\,, \tag{37}$$

that the KH approximation itself is valid. With the same $n = 7$, $l = m = 6$ hydrogen state as an example, Ref. [43] shows that there is no point in continuing the KH solution to $F < F_c$ because the one-photon KH ionisation probability differs significantly from the correct Fermi golden rule value given by Eqn (1).

Application of the Floquet scheme for the Kramers frame to hydrogen Rydberg states in Ref. [44] increased doubts as to whether Eqn (32) is a correct criterion for KH applicability criterion. It was shown, in particular, that stabilisation occurs only at frequencies in excess of the unperturbed Rydberg energy, i.e., at $\omega \gg E_n$. This is entirely

consistent with the conclusions of Ref. [42] cited earlier. At $\omega \sim E_n$ no stabilisation is found, however, which disagrees with the hydrogen ground state results discussed above (in this last case, KH stabilisation occurred also at $\omega < E_1$; see the case $\omega = 0.25$ in Fig. 11).

In summary, in the high-frequency limit the KH approximation appears to be very much justified for $\omega \gg E_n$, where E_n is the unperturbed initial level of the atom. The low ionisation probability values are due to the fact that the N-photon perturbation [Eqn (30)] decreases sharply both with increasing ω [because of the strongly oscillating integrand in Eqn (30)] and with increasing N. The validity of this approximation is also confirmed by comparing it with the direct numerical solution of the Schrodinger equation for a model potential [29] assuming the dichotomy condition, Eqn (37). We saw above, however, that many questions concerning the applicability of the KH approximation still remain.

Nevertheless, the KH approximation is confirmed by direct numerical solution of the time-dependent Schrodinger equation [45]; it can be concluded that in a superintense field oscillations of an electron wavepacket weakly coupled to the atomic core occur. More detailed information on the application of the KH approximation can be found in Ref. [2].

5. Interference stabilisation

A totally different mechanism for the stabilisation of Rydberg states was proposed in the series of studies [46–49] (see also Ref. [50]). A Rydberg electron absorbs a photon of frequency $\omega > E_n$ and moves first into the continuous spectrum. After this it escapes to infinity (ionisation) or goes back to a Rydberg state via the induced emission of an external-field photon. This state need not be the initial one because the absorption and emission are virtual processes and thus do not require that the law of conservation of energy be obeyed. At the next stage, the electron can again absorb a photon, and this process can repeat itself many times (see Fig. 3).

To obtain the total ionisation amplitude, amplitudes for all orders of the perturbation theory must be added together. We will see later that the interference of these partial amplitudes is destructive, so that the total amplitude is (in absolute value) less than any individual component. The ionisation rate decreases with the field in superintense fields — i. e., Rydberg states are stabilised.

We now proceed to the quantitative description of this process, following the presentation given in a book by the present authors [1] (see also an alternative presentation in Ref. [51]). In the first order of the perturbation theory, the matrix element of the bound–free transition is

$$V_{nE} = z_{nE} F \,, \tag{38}$$

where z_{nE} is the dipole matrix element (assuming linear polarisation along the Z axis) and F is the field amplitude.

In the next order we have a three-photon matrix element corresponding to the $n \to E' \to n' \to E$ transition (explicit expressions for multiphoton matrix elements are given in Ref. [15]):

$$V_{nE}^{(3)} = \sum_{n'} \int \mathrm{d}E' \, \frac{V_{nE'} V_{E'n'} V_{n'E}}{(E' - E_{n'} - \omega)(E' - E + \mathrm{i}\delta)} \tag{39}$$

($\delta \to +0$). The integral over intermediate states of energy E' has the principal-value and pole contributions. Neglecting the former for numerical reasons [52] (the so-called pole approximation [53]), from Eqn (39) we find

$$V_{nE}^{(3)} = -\mathrm{i} f(E) V_{nE} \,, \tag{40}$$

where

$$f(E) = \sum_{n'} \frac{|V_{n'E}|^2}{E - E_{n'} - \omega} \,. \tag{41}$$

The next, five-photon matrix element is similar in form to Eqn (40), but with $-\mathrm{i}f(E)$ being replaced by $|-\mathrm{i}f(E)|^2$. Thus, the series from matrix elements to all orders in the perturbation theory is an infinite geometric progression. Its sum is obviously

$$\tilde{V}_{nE} = \frac{V_{nE}}{1 + \mathrm{i} f(E)} \,. \tag{42}$$

Hence, for the Rydberg state with principal quantum number n, on averaging over the remaining quantum numbers, we find the ionisation probability to be

$$\tilde{w}_{nE} = \frac{w_{nE}}{1 + f^2(E)} < w_{nE} \,. \tag{43}$$

Here w_{nE} is the one-photon ionisation rate of the state according to the Fermi golden rule (recall the photon energy is assumed to be larger than the binding energy of the Rydberg state).

It is thus clear that the destructive nature of the interference is due to the use of the pole approximation for matrix elements. If, however, one considers only the principal-value integral in Eqn (39) and similar multiphoton matrix elements, then either destructive or constructive interference is possible (the latter case implying enhanced ionisation).

The critical field E_c for a given Rydberg state is determined by the condition (see the Introduction)

$$w_{nE} t_n = 1 \,, \tag{44}$$

where $t_n = 2\pi n^3$ is the time of revolution of the Rydberg electron around the atomic core. Since the estimated one-photon ionisation cross section for the nth Rydberg state is (Kramers formula, see Ref. [54])

$$\sigma_n \sim \frac{n}{c} \,, \tag{45}$$

the probability of such ionisation is estimated to be

$$w_{nE} = \sigma_n \frac{c F_c^2}{8\pi\omega} \sim \frac{n F_c^2}{\omega} \,. \tag{46}$$

Substituting Eqn (46) into (44) yields the dependence of the critical strength F_c on n for the one-photon ionisation frequency $\omega \sim 1/2n^2$:

$$F_c \sim \frac{1}{n^3} \,. \tag{47}$$

If $F \ll F_c$ then $f \ll 1$ from Eqn (43), and

$$\tilde{w}_{nE} \approx w_{nE} \sim \left(\frac{F}{F_c}\right)^2 \,. \tag{48}$$

If, on the contrary, $F \gg F_c$, then unity may be neglected compared with f^2 in Eqn (43), and since $f \sim F^2$ from Eqn (41), from Eqn (43) we obtain

$$\tilde{w}_{nE} \sim \left(\frac{F_c}{F}\right)^2 \,. \tag{49}$$

Thus, in a superintense field the stabilisation of Rydberg states is of an interference type.

The above argument ignores free–free electronic transitions in the continuum, which involve the absorption and emission of external-field photons. Their inclusion gives a somewhat modified expression for the ionisation rate. In particular, for $F \gg F_c$, instead of Eqn (49) we have [55]

$$\tilde{w}_{nE} \approx \frac{1}{2\pi n^3} \frac{F_c}{F} . \tag{50}$$

The factor $t_n = 2\pi n^3$ has been introduced because at $F = F_c$ we must have $w_{nE}\, t_n = 1$ from Eqn (44).

Moreover, the present approach sets an upper limit on the field strength F. In order to be able, in accordance with Fig. 3, to speak of Rydberg orbits to which the electron returns periodically on emitting a photon, the orbits must not be distorted too much — not to the point of dumbbell 'dichotomy' (see above). As we saw in the beginning of this section, this requires that the electron oscillation amplitude $a = F/\omega^2$ be small compared with the size of the Kepler orbit, which is n^2, so that at $\omega \sim 1/n^2$ we have

$$F \ll \frac{1}{n^2} . \tag{51}$$

Inequality (51) does not imply that the field may still be superintense in the sense of Eqn (47), because $1/n^3 \ll F \ll 1/n^2$ for $n \gg 1$.

So far we have discussed (within the interference stabilisation context) only the imaginary part of the energy of the ionised state — i. e., the ionisation rate. We turn next to the change in the real part of the energy of a Rydberg state in a superintense field, i.e., we will consider the Stark shift of the level. A model adopted in Ref. [49] involves two adjacent Rydberg levels, n and $n+1$, coupled via the external field through one-photon transitions to the continuum and back (see Fig. 3). It is shown that in a superintense field a narrow quasi-energy state (i. e., that of the system 'atom + field') appears, which lies exactly halfway between the unperturbed Rydberg states whose widths decrease with increasing field strength. A similar picture is obtained for a large number of equidistant Rydberg levels [55]: in a superintense field, narrow quasienergy levels lie exactly midway between the unperturbed Rydberg levels.

As regards the critical field in this model, the following remarks can be made concerning the estimate (47) above. This estimate was obtained by assuming that the Rydberg atom ionises within approximately one Kepler orbit. However, if one considers a Rydberg state with a given n and a low orbital quantum number l, and if one does not average over l — as is valid for complex atoms with large quantum defects — then the matrix elements of classical bound–free transitions [56] should be employed. Then, within the present interference stabilisation model, the critical strength is determined from the condition $f = 1$, where f is given by Eqn (41). This yields [50]

$$F_c = \omega^{5/3} \sim n^{-3.33} , \tag{52}$$

which is close to but somewhat different from Eqn (47). This correction does not rule out the possibility of a (superintense) field range for which the above analysis is correct [see Eqn (51)].

The quasiclassical matrix elements of Ref. [56], which allow us to go over from Eqn (47) to Eqn (52), are justified only for low values of initial orbital quantum numbers for which $(\omega l^3)/3 \ll 1$. This restriction has practical significance in that in the visible range it often leads to the rather restrictive inequality $l \lesssim 2$. Numerical calculations show that, as l increases, bound–free matrix elements decrease rapidly. This results in large critical strengths F_c for large l values.

Very similar results are obtained in a formulation [57] in which Volkov wave functions are constructed for an electron in a Kepler orbit with the quasiclassical approximation to account for the Coulomb core potential. This formulation employs the result [58] that quasiclassical bound–bound and bound–free matrix elements between low orbital quantum number states are dominated by the region in which the distance of the electron from the atomic core is of order $r_q \sim n^{4/3}$, which is small compared with n^2, the scale of the quasiclassical electron motion. The ionisation probability calculated from this wave function also displays stabilisation as a function of the external-field strength (see Ref. [59] for details).

In the above analysis one of the Rydberg states was assumed to represent the initial condition of the problem. In reality, however, the initial state is produced from the atomic ground state by an electromagnetic field. Since the field is a laser pulse with a certain spatiotemporal distribution, not a single Rydberg state, but in fact a Rydberg wavepacket may be excited. The shape of the laser pulse has been shown [48] to be crucial in determining the dispersion of the wavepacket. For a long pulse $t_l > 2\pi n^3$, where n is the principal quantum number of the Rydberg state, the ground-state multiphoton ionisation is predicted [60] to be strongly suppressed via resonances with Rydberg states with subsequent one-photon ionisation. The reason for this is the stability of the Rydberg wavepacket against further ionisation.

An analytical solution exists for the ionisation of the quasicontinuum of Rydberg states excited from the ground state resonantly by a trial field [61–62]. The solution confirms that an atomic system becomes stable for ionisation when the ionisation width is much greater than the spacing between the Rydberg states.

To summarise the above discussion of interference stabilisation studies, note that all of them rely on the pole approximation for the bound–free and free–free multiphoton matrix elements [see the argument leading from Eqn (39) to Eqn (40)]. The numerical arguments underlying this approximation are by no means valid for all matrix elements, and its justification would therefore be a strong argument in favour of the present model. There are two further points that need careful analysis: (1) the Stark splitting of n Rydberg states into components with different values of l and the magnetic quantum number m; and (2) the possibility of interference stabilisation being caused by coupling of the Stark multiplet components via the continuum because of the Raman scattering of the external field. This is quite a challenging problem because matrix elements between states with widely different magnetic quantum numbers may be very small, or it may not be possible to excite some of these states at all because of selection rules for a given radiation polarisation. Therefore, even though the energy intervals between the initial states with different n are filled with a large number of substates with different orbital and magnetic quantum numbers, the substates may remain unbroadened, i.e., no quasicontinuum may occur. Thus criterion (52), which is often used to

assess the possibility of interference stabilisation, is not in fact realistic (Rydberg states are Stark-split!) but rather corresponds to a simple no-splitting model. Increasing the radiation frequency also prevents the formation of a quasicontinuum by decreasing the matrix elements for many of the transitions involved.

Interference stabilisation itself is a very general principle which emerges as a consequence of the quantum interference phenomenon. If, on the contrary, there is one lower state and two close upper states, then the monochromatic resonant electromagnetic field will generate a dipole moment for either of the transitions. The phase relation between the two dipoles depends on resonance detuning. If the dipoles are equal in amplitude and opposite in phase, the total dipole moment is zero.

6. Stabilisation of classical systems

So far we have discussed the behaviour of quantum-mechanical systems in a superintense electromagnetic field. In this section, the work on the dynamics of classical systems in such fields will be reviewed. In a sense, the Rydberg states discussed in the preceding section may exemplify classical systems, although in some cases the quasiclassical and classical pictures disagree for large times because of the spreading of quantum-mechanical wave-packets.

Needless to say, classical stabilisation is much easier mathematically because what we solve here is Newton's equation in a time-dependent external field instead of the Schrodinger equation in the quantum case. For the Coulomb problem, the Newton equation takes the simple form of (we set $e = m_e = 1$ from this point on):

$$\frac{d^2\boldsymbol{r}}{dt^2} = -\frac{\boldsymbol{r}}{r^3} + \boldsymbol{F}\cos(\omega t + \varphi) \ . \tag{53}$$

Here a linearly polarised field is assumed for the sake of definiteness. Also, some initial conditions — for example, at the time $t = 0$ corresponding to the initial finite electron orbit — are specified.

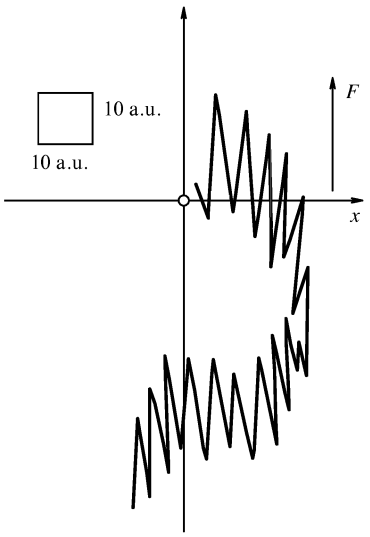

Figure 13. Example of a quasistable trajectory for the excited $n = 3$ hydrogen state perturbed by a field with a frequency $\omega = 0.15$ a.u. and amplitude $F = 0.4$ a.u. (linear Z polarisation). Calculations are taken from Ref. [63].

The numerical solution of Eqn (53) in Refs [63–65] demonstrates the existence of stable electron trajectories in a superintense field (Fig. 13). The electron oscillates around the atomic core with the frequency ω and amplitude $a = F/\omega^2$ along the normal to the plane of the orbit, and at the same time performs a distorted Kepler motion in the plane of a highly eccentric orbit. The motion of the electron remains finite (which means stabilisation), although the oscillatory energy $F^2/4\omega^2$ is large compared with the unperturbed binding energy $E_n = 1/2n^2$ of the electron.

Ionisation from such trajectories occurs only when the electron approaches the nucleus to within a small distance r_0 such that the Coulomb energy $1/r_0$ and the interaction of the electron with the field (Fr_0) are of the same order [see Eqn (4)]:

$$r_0 \sim F^{-1/2} \ . \tag{54}$$

Since $F \gg 1/n^4$ for a superintense field with a frequency which is not very high, we have $r_0 \ll n^2$, i.e., the electron must approach the nucleus to within a small distance compared with the size of the Kepler orbit, $\sim n^2$. This happens rarely because generally, owing to large oscillations at the time the electron passes close to the nucleus, the effect of three dimensionality is that the electron finds itself far from the nucleus along the normal to the orbit plane. It is this occurrence which is at the origin of the stabilisation of a classical system.

Calculations show [63] that stabilisation depends significantly on the phase φ in Eqn (53) which corresponds to the field being turned on at time $t = 0$. Numerical calculations predict stable trajectories only for $\varphi \approx 0$. The initial electron velocity is in this case zero according to Eqn (53). If $\varphi \neq 0$, the nonzero initial velocity causes a fast escape of the electron to infinity — which is ionisation. A smooth turn-on of the superintense field is another way to prevent the electron from moving away from the nucleus initially, but in this case the turn-on process passes through atomic field values, at which the ionisation probability is high. So in actual fact stabilisation can be achieved only by optimising the problem parameters in some way.

In Ref. [66] the frequency dependence of the ionisation probability was investigated for the classical hydrogen atom at fields up to $F = 5$ a.u. It is found that the stabilisation effect occurs only at high frequencies $\omega > 40$ a.u. Below these frequencies, the main ionisation channel at superintense fields involves escape directions perpendicular to the field polarisation vector.

The Coulomb potential used in Eqn (53) has a singularity at the origin. If the singularity is smoothed out, the atomic potential becomes more transparent for the electron and hence the ionisation probability — the strength of the superintense field being the same — decreases. This is because of the fact that the interaction of the electron with the nucleus near this latter field becomes weaker, and it is this interaction, as we saw above [see Eqn (54)], which causes the electron to escape to infinity in a superintense field.

Numerical calculations [67] support the above argument for a one-dimensional smoothed Coulomb potential of the form

$$V(x) = -(x_0^2 + x^2)^{-1/2} \ . \tag{55}$$

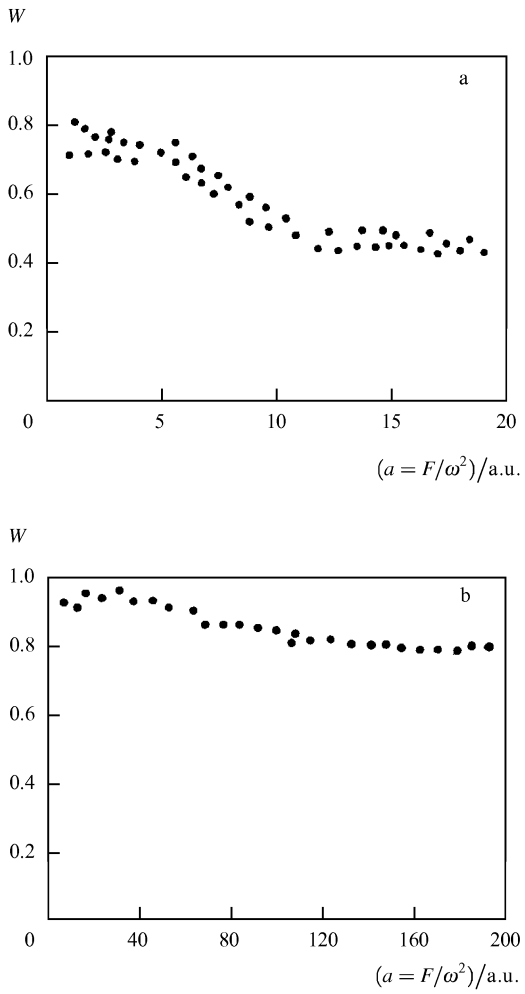

Figure 14. Probability of ionisation in a one-dimensional Coulomb potential [Eqn (55)] as a function of the electron oscillation amplitude in an electromagnetic wave field, $a = F/\omega^2$; taken from the calculations of Ref. [67]. Field frequency is $\omega = 0.8$ a.u.; the smoothing parameter x_0 in the potential [Eqn (55)] is 1 in the case (a) and 0.1 in (b).

In Fig. 14 the total ionisation probability for the atomic potential [Eqn (55)] with $= 0.8$ a.u. is shown as a function of the electron oscillation amplitude $a = F/\omega^2$ for (a) $x_0 = 1$, and (b) $x_0 = 0.1$. The pulse length is 50 field cycles. It is seen that in the first case the stabilisation effect is larger than in the latter — especially if one notes the difference in abscissas between (a) and (b). Thus, the more singular the atomic potential, the smaller the super-intense stabilisation, all other parameters of the problem being the same.

We next examine how the stabilisation of a real 3D hydrogen atom depends on the orbital quantum number l — i.e., on the Kepler orbit eccentricity — of the initial state. From our preceding discussion, one would expect that, all other things being equal, circular orbits are harder to ionise because finding the electron near the origin (nucleus) is a rare event, and the coordinate values of Eqn (54) are difficult to obtain. This argument was supported by numerical calculations [68]. In particular, for a CO_2 laser and for $n = 50$, $l = 30$ Rydberg states, even at the field strength $F = 3 \times 10^4/n^4 = 2.5 \times 10^7$ V cm^{-1} ionisation is completely absent for 5000 field cycles. These results, however, are only for $m = 0$ (the projection of the orbital moment on the direction of polarisation is zero). In this case, there is actually no stabilisation of the type discussed above: the ionisation probability is zero up to a certain critical field strength F_c and equals unity above. Interestingly, the critical value is tens of thousands of times the atomic field.

If $m \neq 0$, then a collision of the electron with the nucleus is easier to avoid than for $m = 0$ because in this latter case the electron oscillations in the electromagnetic wave field occur in the plane of the unperturbed Kepler orbit (assuming linear polarisation). It is therefore not surprising that in the $m \neq 0$ case the ionisation probability decreases with the strength of the linearly polarised field [69] — which indicates stabilisation. This of course happens at much stronger fields than those needed for diffusion-assisted atomic ionisation [70]. The scale of the field strength for the classical diffusion of the electron via the Kepler orbits is set by

$$F_D = \frac{1}{50n^4(\omega n^3)^{1/3}} . \tag{56}$$

It is seen that because of the large numerical factor in the denominator, the result is much below the critical strength estimates given above.

Classical calculations for other potentials confirm the conclusions made above. Reference [71], for example, employed the potential

$$U(x_1, x_2) = -2(x_1^2 + 1)^{-1/2} - 2(x_2^2 + 1)^{-1/2} + \left[(x_1 - x_2)^2 + 1\right]^{-1/2} , \tag{57}$$

corresponding to the classical one-dimensional helium atom with a smoothed Coulomb interaction. The calculations were made in the KH approximation (see Section 4), applicable not only to the Schrodinger equation as in the previous discussion, but to Newton's equation as well. Even for a superintense field, the 'dichotomy' phenomenon takes place. In a superintense field of high frequency ω, two-electron stabilisation with the electrons on the opposite sides of the nucleus is observed [71]. A similar conclusion is reached in three dimensions. The effect of stabilisation occurs at intensities above 10^{18} W cm^{-2} at $\omega = 4.5$ a.u. It is also shown that under the stabilisation conditions the electrons find themselves at classical turning points $a = \pm F/\omega^2$, and that even in three dimensions their motion is in fact one-dimensional — in the direction of the external-field polarisation vector. All in all, the above survey leads to the conclusion that the effect of stabilisation takes place not only in quantum but also in classical mechanics. Also, both approaches are similar in the way the ionisation probability depends on the unperturbed orbit parameters (electron energy and momentum) and the momentum projection depends on the polarisation direction. Clearly, in classical mechanics we are dealing with an electron escaping beyond the laser radiation pulse and cannot speak of ionisation probability as we can in quantum mechanics. Also, classical calculations demonstrate more clearly that it is necessary to smooth out the Coulomb potential at the origin in order to avoid mathematical difficulties due to infinite quantities.

7. Experiment

Before we proceed to the experimental data, a few preliminary remarks are in order.

First, modern laser technology does not allow ground-state stabilisation experiments. In fact, from the basic

theoretical arguments presented above, such stabilisation requires ultraviolet radiation ($\omega > E_0$) with a critical intensity in excess of the atomic value ($I_c \gg I_a$). Also, to be able to pass through the 'death valley' at the pulse front at $I \sim I_a$, the front time t_f must be of the order of the atomic time ($t_f \sim 10^{-16}$ s). Only at $t_f < t_a$ will a significant part of atoms remain not ionised during the pulse rise time of order t_a for $I \sim I_a$, and retain their initial state until the pulse peak is reached, whereas at $I_c \gg I_a$ the stabilisation effect should be expected. To satisfy all the three requirements simultaneously is not yet possible. While the progress in laser technology should be expected to fulfil the first two requirements in the near future, the third appears to be unachievable, even with the newly developed method which enables the distribution of temporal radiation to be controlled by selection of an appropriate spectral radiation profile.

Therefore all present-day experiments make use of excited atomic states. For these, all the three conditions mentioned above apply although numerically they are much less strict. The photoionisation channel condition $\omega > E_n$ may be fulfilled not only for the visible frequencies but — for highly excited (Rydberg) atoms — even in the infrared. In the latter case, the critical intensity is much lower than the atomic value, $I_c \ll I_a$. The sharp dependence of the atomic time on n ($t_{an} = n^3 t_a$) allows one to pass the 'death valley' effectively at large n by using ultrashort pulses with rise times of the order of picoseconds or femtoseconds.

Another point to note is that, at the time of writing (the autumn of 1995) this paper, no reported experiment has provided unequivocal evidence for, and a sufficiently complete picture of, the stabilisation effect. The different experimental results to be discussed below agree only partly with theoretical predictions, leaving quite a few questions unanswered.

Third, under experimental ground-state stabilisation conditions some other effects may occur, which also suppress photoionisation but have nothing to do with stabilisation. These should be taken into account and distinguished clearly in investigating the stabilisation effect. In some cases, it is these effects which determine the optimal design of a stabilisation experiment. However, these 'ionisation suppression' effects are of obvious interest by themselves from the point of view of the physics of intensive coherent radiation interacting with an atom.

Finally, it should be kept in mind that, whatever the experimental arrangement, one can measure the total photoionisation yield only after the target has been exposed to a laser pulse with a fixed, inhomogeneous spatiotemporal distribution. Under such conditions, photoionisation rate data can be obtained only by measuring and taking into account the spatiotemporal radiation distribution. The influence of the inhomogeneity of this latter can be reduced by various methods, but the inhomogeneity always remains. Apart from the necessity to account for the radiation distribution, various effects due to finite pulse length and inhomogeneous distribution may occur. A case in point is the pulse length comparable with the Kepler period of the Rydberg electron. This situation occurs for picosecond and femtosecond pulses for $n \gg 1$ Rydberg states (the effect of pulse length will be discussed later). Another example is related to the necessity of passing the 'death valley' at the rise of the pulse. This situation is encountered when photoionisation is observed at an atomic-scale pulse-peak field strength: it is necessary that during the rise time of the pulse, within the time interval when $F \sim F_a$ — i.e., in the 'death valley' — only a small fraction of the atoms be ionised. Obviously, to pass effectively the 'death valley' is possible only if the rise time is of the order of the Kepler period or less — which actually implies Rydberg atomic states.

We now proceed to a discussion of the experimental data by taking specific experimental arrangements as the basis for the analysis. We must first discuss some effects which suppress photoionisation but have no relation to the stabilisation effect.

7.1 Photoionisation suppression effects

There are a number of effects that suppress photoionisation but do not involve stabilisation. These effects are contingent on a quite specialised experimental arrangement and are of obvious interest by themselves. So far as the study of stabilisation is concerned, they indicate the initial conditions that hamper optimal stabilisation experiments.

One photoionisation suppression effect is illustrated nicely by the simple example of a classical electron rotating in a Kepler orbit around the nucleus. If the orbit is a highly eccentric ellipse, the absorption of a photon and the detachment of the electron may occur only at moments when the electron is close to the nucleus in its orbital motion. If the length t_l of the photoionising pulse is less than the Kepler period, the process of photoionisation will be suppressed because the electron may not come close to the nucleus during the time the radiation acts on the atom.

In practice, such suppression may occur only in the photoionisation of excited states, for which the Kepler period $t_{an} = n^3 t_a$ may exceed the pulse length t_l. It is seen that even at $n = 10$ we have $t_{an} = 10^{-13}$ s, which is comparable with the length of an ultrashort pulse.

Such an effect was observed in a study [72] of photoionisation from highly excited states of barium. The $27d$ state was excited out of the ground state by a standard two-step method with radiation from two dye lasers. The Kepler orbit time for the $27d$ state is $t_{a27} = 2$ ps. From this excited state, the atom was photoionised by radiation with pulse length t_l which varied from 2.7 to 0.3 ps. The result is shown in Fig. 15. Three

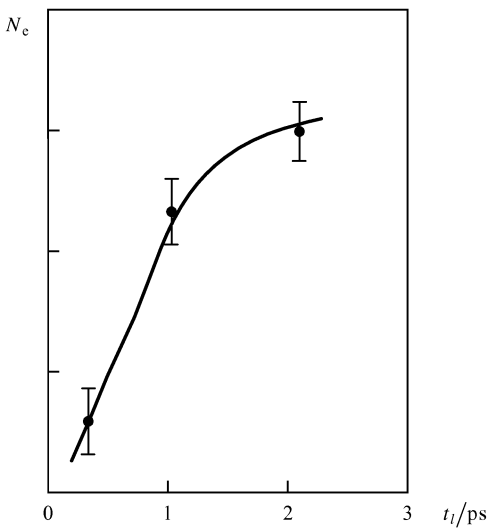

Figure 15. Photoelectron yield N_e from the $27d$ barium state versus laser pulse length t_l in the experiment described in Ref. [72].

regions showing different pulse-length dependences of photoionisation yield are distinguished. At $t_l > t_{a27}$ the yield is pulse-length independent, at $t_l < t_{a27}$ it decreases with decreasing pulse length, and at extremely short pulses an approximate proportionality is observed. The results are interpreted classically, in terms of the probability for finding the electron close to the atomic core during the laser pulse.

Thus, this experiment demonstrates the suppression of photoionisation at pulse lengths less than the Kepler revolution of the electron around the atomic core.

In another suppression effect, the initially excited state is the $n \gg 1$, $l \sim 1$ state. It is obtained by the standard cascade (step) excitation method with the linearly polarised radiation from several dye lasers. As a strong, external high-frequency ($\omega > E_n$) ionising field is turned on, the initial $n \gg 1$, $l \sim 1$ state splits into $n-1$ components with l varying from 0 to $n-1$ (see, e.g., Ref. [15]). The splitting is quadratic in the field and described by a perturbative formula of Ref. [73] (see also Ref. [74]) which shows it to be dependent on all the quantum numbers of the initial state as well as on the frequency and strength of the field. In the laser radiation field, the manifold of the split states forms a wavepacket. The dynamics of this latter involves its oscillations around the atomic core, the period of which is determined by the splitting $t_{osc} = 2\pi/\Delta_p$ and by the spreading during a time period dependent on laser monochromaticity. If the pulse length of the ionising laser is less than the packet oscillation period, then the photoelectron yield will be suppressed because during the laser pulse no low-l states may exist near the atomic core. As is known, the ionisation probability from high-l states is suppressed compared with low-l states because of the large momentum the free electron must have in the former case. The results of a model experiment [75] with Rydberg levels split in a static electric field agree well with the models discussed above.

Photoionisation suppression due to the splitting of excited atomic levels in a static electric field was observed in an experiment on barium [76]. The states studied were $n = 25$ and $n = 35$, the static field was about $U_1 = 250$ V cm^{-1}, and the strong laser field had the frequency $\omega > E_{35}$, E_{25} (Fig. 16).

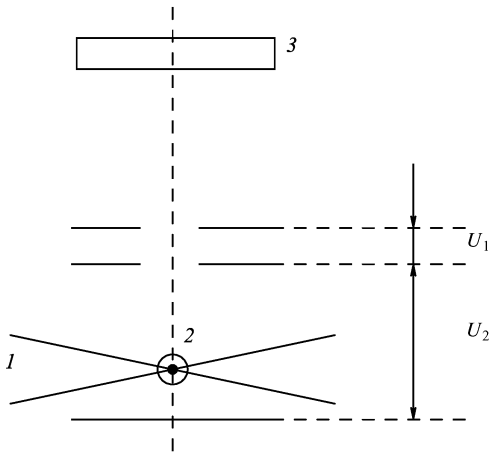

Figure 16. Schematic diagram of the experiment described in Ref. [76]: (*1*) focused laser radiation; (*2*) atomic beam, with the axis perpendicular to the sheet; (*3*), ion detector; U_1 and U_2, constant voltages indicated in the text.

The Ba^{+*} ions generated from the one-photon ionisation of excited barium atoms by the laser radiation were accelerated by a static electric field of about 250 V cm^{-1} and recorded at a microchannel detector. Some of the excited atoms remained in the region where the radiation interacted with ground-state atoms; after the pulse, these atoms drifted into the region with a field of about $U_2 = 4000$ V cm^{-1} and there were ionised by this field. These ions came to the detector at a different time than the Ba^+ ions, owing to one-photon ionisation. The number of these ions gives information about the residual population of the excited barium atoms after the passage of the pulse.

The net result of the experiment is that the number of ions from $n = 25$ is an order of magnitude less than that from $n = 35$, which shows that the residual population of the latter state dominates and that photoionisation is suppressed.

The interpretation given in Ref. [76] is as follows. The magnitude of l splitting is estimated to be $\Delta_p \sim n^{-4}$ since $U_1 = 250$ V cm^{-1} is close to the estimate n^{-5} for the field at which the (extreme) multiplet components from the nth level are found to cross those from the adjacent levels. Consequently, the estimate for the wavepacket oscillation period, $t_{osc} \sim 1/\Delta_p \sim n^4$, is 60 ps for $n = 25$ and 230 ps for $n = 35$. Since the pulse length was 70 ps, it follows that in the latter case $t_1 \ll t_{osc}$ and hence photoionisation suppression should occur — which indeed did happen in the experiment.

In order for experiments to be free from splitting of Rydberg states, the preliminary excitation must occur into so-called circular states, ones in which, given the value of n, the orbital quantum number assumes its maximum value $l = n - 1$. Clearly, the magnetic quantum number will then be the same, $m = l$. Of the many techniques available for excitation into such states [77–79], multiphoton excitation by circularly polarised radiation [77] is the simplest. In its application, however, the values of n (and hence l) must be relatively small since, with the multiphoton processes involved, effective excitation necessitates large radiation intensities, with all the consequences that may ensue.

7.2 Atomic stabilisation in multiphoton resonant ground-state ionisation

In principle, the high-field stabilisation of an excited atom is not limited to the experimental situation in which weak auxiliary laser radiation is used to excite the atom. The strong field alone may be sufficient if it gives rise to multiphoton resonant ionisation from the ground state of the atom. Since even the stabilisation of excited atoms implies high intensities, the design of such experiments avoids the choice of a radiation frequency for multiphoton excitation. A strong external field always causes a large AC-Stark shift [80], which detunes no-field resonances and produces a host of dynamic resonances on the rising and falling edges of the pulse. Such dynamic resonances have repeatedly been seen in multiphoton ground-state ionisation experiments as resonant peaks in the energy spectrum of the resulting electrons (see, e.g., Refs [80–81]), each individual peak being identifiable with specific excited states of the atom. However, until recently it has never been thought that, in addition to multiphoton resonant ionisation, the dynamic multiphoton resonances may also produce multiphoton excitation, when the atom can, with some probability, remain in its excited state after the pulse. This certainly has not seemed realistic for inert gases under

visible and infrared radiation, when high-order multiphoton processes ($K = 10$) are involved; such processes were observed only in very high fields of the order of $(10^{-2} - 10^{-1})F_a$, but even to excite the lowest states requires about the same number of photons. Only recently has an experiment [82] unexpectedly shown that residually populated excited states may occur in strong-field ground-state multiphoton ionisation.

In that experiment, two laser radiation fields were employed. In one (strong) field, the seven-photon ionisation of the xenon atom was realised ($\omega = 2$ eV, $I = 10^{13}$ W cm^{-2}, $t_l = 100$ fs). The second—trial (and weak)—field was turned on with some delay after the strong field pulse. The trial field parameters were taken as follows: $\omega = 2$ eV, $I = 10^{11}$ W cm^{-2}, $t_l = 5$ ns. The electrons produced by the strong field alone, and those by the two fields together, were detected. The electrons due to the weak (trial) field were separated as a difference effect. Simultaneously, the energies of the produced electrons were measured, in order to provide an independent method to separate the trial-field electrons. A large number of these excited ionisation electrons were found. The electron energy spectrum displayed narrow peaks distinctly identifiable as being due to the excited $4f$, $5f$, and $6f$ states. After a strong field pulse, 11 % of the atoms remained in the excited $4f$ state; 25%, in $5f$; and 56%, in $6f$.

Now the question arises as to the physical reason for the excited-state residual population in the ground-state multiphoton ionisation of xenon. Experimental data and simple estimates show that stabilisation does not play a role in this case. In fact, with the above parameters, typical of powerful laser radiation, the free-electron oscillation amplitude is readily estimated to be $a \sim r_a$, so that the necessary condition for adiabatic stabilisation, $a \gg r_{a5} \approx 10^2 r_a$ (see Section 3 above), is not met. As regards interference stabilisation, the condition $F \gg F_c$, where $F_c = \omega^{5/3}$, is also not realised. Moreover, the narrow resonance peaks in the electron spectrum (Fig. 17) show directly that no quasicontinuum arises from the excited $n = 5$ states. It is thus clear that interference stability is also absent.

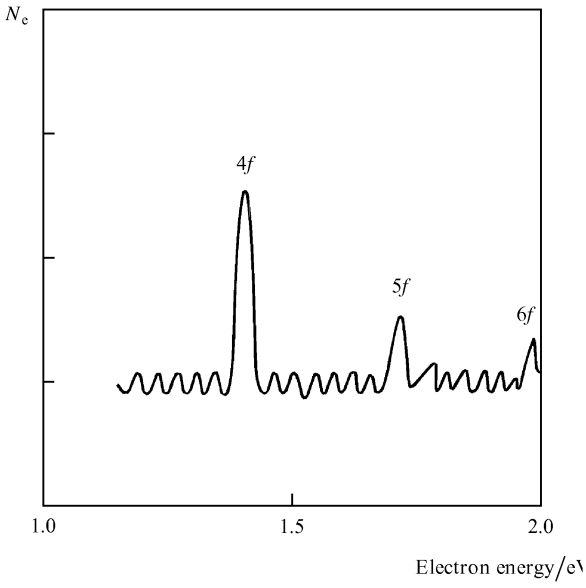

Figure 17. Electron energy spectrum for photoionisation of excited xenon atoms by trial radiation, experimental data are taken from Ref. [82].

Presumably, the residual population is due to the ultrashort pulse length ($t_l = 100$ fs) of the laser used. Estimates show that the ionisation lifetime of excited xenon states in the intense ionising laser field is of the order $t_i = 10^{-13}$ s, which is equal to the pulse length of the laser. Clearly, the total ionisation from an excited state implies $t_l \gg t_i$, and at $t_l \sim t_i$ a large part of the excited atoms must survive. This is another example of a stabilisation-unrelated photoionisation suppression effect.

However, in later work [83] residual population in multiphoton ground-state krypton ionisation was observed under conditions where, on the one hand, it cannot be associated with the short pulse length and, on the other, it may be due to the interference stabilisation effect. Moreover, direct experimental evidence for stabilisation is found.

The strong ionising laser field in Ref. [83] had a frequency $\omega = 1.5$ eV, pulse length $t_l = 100$ fs, and peak intensity $I = 5 \times 10^{15}$ W cm^{-2} (field strength $F = 2 \times 10^9$ V cm^{-1} $\approx 0,5 F_a$). The ions produced in the laser focus region were accelerated to the detector by a 100 V cm^{-1} static electric field pulse. After the pulse, a pulsed electric field of a few thousand volts per centimetre was applied across the ion formation region, sufficient to ionise excited atoms in $n \geqslant 14$ states. By varying the strength of the field, conditions for ionising excited atoms in states from $n = 50$ up to $n = 14$ were realised. The ions produced by the pulse and those produced by the static field strike the detector at different times. The static field ions signalled the existence of residual population after the laser radiation pulse.

The experimental data of Ref. [83] show that after the pulse about 1 % of the atoms remain in $n \geqslant 14$ excited states.

We turn next to the interpretation of this experiment.

The first thing that has to be said is that, given the experimental conditions used, the residual population cannot be attributed to the short pulse length. In fact, for the peak field strength mentioned above, any estimate yields $t_i \ll t_l$ for the ionisation lifetime of excited atoms with principal quantum numbers from 14 to 50.

A second point is that the residual population of excited states may be due to the stabilisation effect. The adiabatic stabilisation mechanism is of no relevance here. Estimates show that, even at the peak of the laser pulse, the free-electron oscillation amplitude $a = F/\omega^2$ is only about the size of the excited-state orbit $r_{an} = n^2 r_a$ at $n \geqslant 14$. Thus, the condition for the occurrence of adiabatic stabilisation is not fulfilled (it requires $a > r_{an}$). On the other hand, the laser field is much stronger than the critical value for interference stabilisation to occur, $F_c = 0.005 F_a$. However, the principal argument in favour of interference stabilisation is the dependence of the number of excited states on the radiation field strength (Fig. 18). These results show that a fourfold change in intensity leaves this number virtually unchanged. This dependence is typical of the stabilisation effect. The observed increase in the number of excited atoms as the radiation spectrum is broadened (i.e., the pulse length decreases) is presumably because of the suppression of ionisation under conditions where $t_l < t_{an}$, where t_{an} is the time of the Kepler orbit time of the excited electron (for $n = 14$, $t_{an} \sim 10^{-12}$ s). This effect has been discussed earlier in this review (see Section 2).

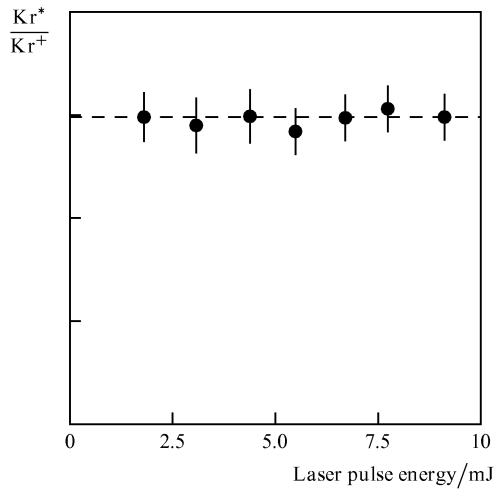

Figure 18. Ratio of excited Kr^* atoms to Kr^+ ions as a function of laser pulse energy. Experimental data are taken from Ref. [83].

Thus, the experimental results of Ref. [83] are in our view in general agreement with the theoretical predictions concerning atomic interference stabilisation (see Section 5), and it is not clear why the authors of that study failed to exploit the effect to interpret their results.

7.3 Stabilisation effect in photoionisation from highly excited states

In Section 5, the model of the interference stabilisation of highly excited states assumed the absorption and subsequent emission of photons by an atomic electron in a strong external field. This multiphoton process is Raman type and may occur in the case when, owing to the ionisation broadening of the atomic levels, the initial discrete spectrum becomes a quasicontinuum. The interference of reradiation processes then turns out to be destructive, leading to a suppression of photoionisation from these states—i.e., to the so-called interference stabilisation of the atom. Since Rydberg states initially with a principal quantum number n split into components with different orbital quantum numbers l in a high-frequency ($\hbar\omega > E_n$) field (see, e.g., Ref. [15]), the splitting can also lead to photoionisation suppression under certain conditions.

As of the time of writing, three experiments on interference stabilisation have been reported.

The experiment in Ref. [84] deals with the photoionisation from the highly excited barium state $6s26d$ induced by radiation of frequency $\omega = 2$ eV, pulse length $t_l = 100$ fs, and peak intensity $I = 4 \times 10^{12}$ W cm^{-2}. One result (Fig. 19) is that, in the presence of a strong field, photoionisation not only from the initial state $26d$, but also from a number of adjacent states up to $31d$ is observed. This is attributed to the initial $26d$ population being Raman redistributed over the adjacent Rydberg states. It is also argued that Raman transitions occur through the continuous, rather than the bound-state, spectrum (Fig. 20). This follows from the experimental fact that the number of repopulated states does not depend on the laser frequency, the range of which (about 300 cm^{-1}) is an order of magnitude more than the separation between the excited states. Clearly, a change in frequency changes the detuning from quasiresonances in the bound-state spectrum and

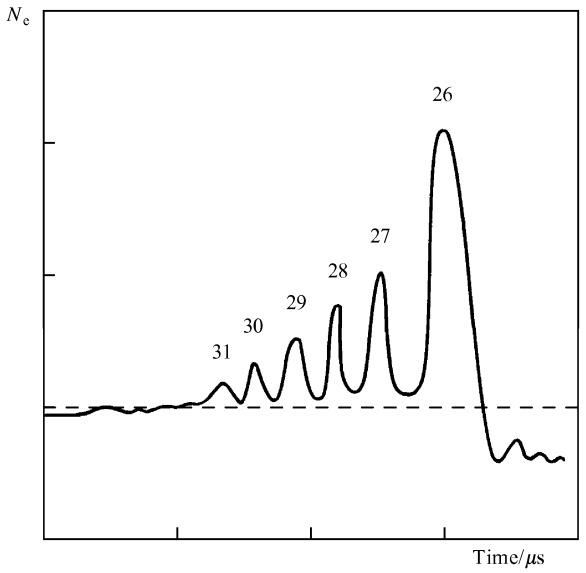

Figure 19. Electron spectrum for the photoionisation of the $26d$ barium state by an intense laser field. The experimental data are taken from Ref. [84].

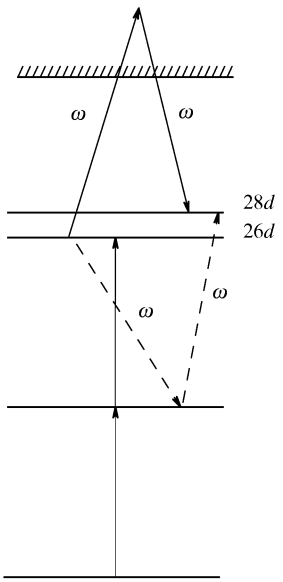

Figure 20. Scheme of two possible channels for two-photon Raman transitions: via the continuum (——) and via the spectrum of bound states (- - - -) [84].

should therefore influence the excited-state repopulation probabilities.

Basically, these results are a direct demonstration of highly excited states being coupled via Raman transitions through the continuum. A detailed theoretical discussion of this process is given in Ref. [62] (see Section 5).

The experiment in Ref. [76] has already been considered above to illustrate the photoionisation suppression due to the l splitting of highly excited states. We will discuss it here from the point of view of stabilisation. As already mentioned, the main result of this experiment is that photoionisation from different l components of the highly excited $n = 25$ and $n = 35$ barium states reveals these states to be populated residually after the laser pulse, the second

state being about an order of magnitude greater than the first. The interpretation was presented earlier and has nothing to do with the stabilisation effect. However, for $\omega = 3.5$ eV used in that experiment, the critical field for the existence of a quasicontinuum in the region of highly excited states with a given n is

$$F_c = \omega^{5/3} = 3 \times 10^{-2} F_a = 1.5 \times 10^8 \text{ V s}^{-1} ,$$

corresponding to the radiation intensity $I = 2 \times 10^{13}$ W cm^{-2}. From Ref. [76], the peak intensity in the experiment was about 10^{14} W cm^{-2}. Thus, the interference stabilisation condition was satisfied. Actually, however, each n state was split into components with different values of l in a static field. Accordingly, the critical strength for the existence of a quasicontinuum could be less in this case. This supports the conclusion about the necessary conditions for interference stabilisation. We also note that the value 10^{14} W cm^{-2} is open to criticism, as one resulting from estimates rather than from exact measurements.

Now an obvious question here is whether the results of this experiment are consistent with the concept of stabilisation?

One result, already mentioned in Section 7.1, is that the number of atoms which remain in the excited state after the passage of the pulse is an order of magnitude larger for the $n = 35$ than for the $n = 25$ initial state. As the basic condition $F > F_c$ is fulfilled in both cases, this discrepancy finds no explanation within the interference stability framework.

Another result is the discrete frequency dependences of the yield of Ba^+ and Ba^{*+} ions (Fig. 21). Here Ba^{*+} denotes a barium ion from an excited atomic state. Both dependences display a sparse structure, for ionisation from a fixed n various l manifold, and a finer one, for ionisation from individual fixed n fixed l states. This picture suggests the absence of a photoionisation continuum both for states with different l and for those with fixed n and l values. But the idea of the discrete spectrum being replaced by a continuum is fundamental to the theory of interference stabilisation.

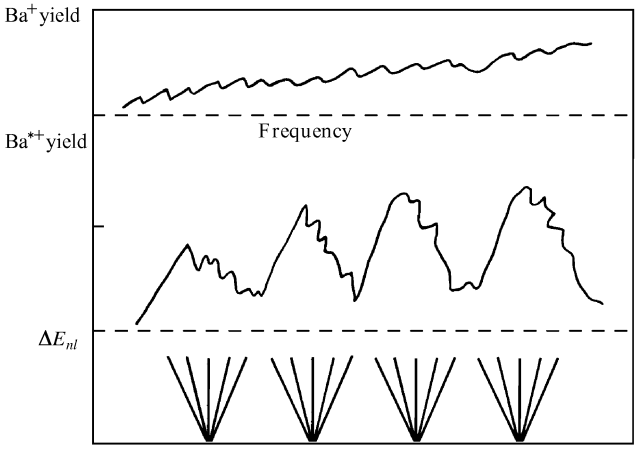

Figure 21. Yield of Ba^+ ions (produced from the ground state) and of Ba^{*+} ions (produced from an excited state) against the radiation frequency [76]. Bottom: splitting of highly excited states with a fixed principal quantum number n into various orbital quantum number (l) components (calculation).

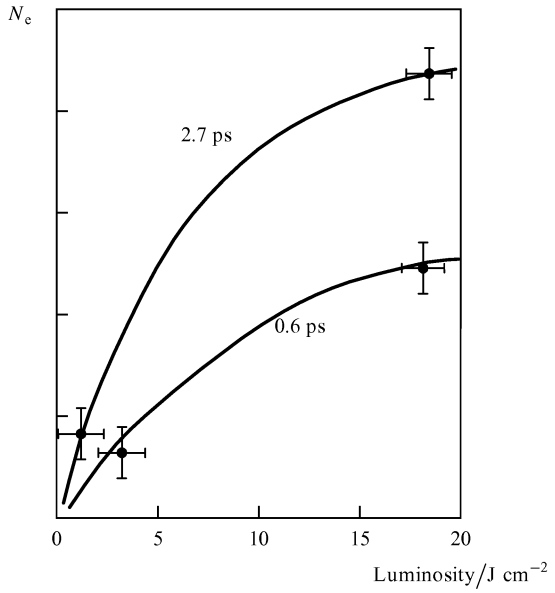

Figure 22. Photoelectron yield from the 27d barium state versus fluence for two pulse lengths. Experimental data are taken from Ref. [72].

Thus, the results of this experiment are inconsistent with the basic theory of interference stabilisation.

The fulfillment of the condition $F > F_c$ does not actually contradict these results: the authors of the experiment give 10^{14} W cm^{-2} as an estimate for radiation intensity, whereas the true value might be much less. This assumption is in accordance with experimental fact and confirms the photoionisation suppression effect due to the l splitting of Rydberg states.

Finally, only a part of the experiment in Ref. [72] has been discussed above (Section 7.1). Also presented in the work are the illumination dependences of the photoionisation yield for the highly excited state 27d for two pulse lengths, 0.6 ps $< t_{an}$ and 2.7 $> t_{an}$, where t_{an} is the period of revolution of the electron for the $n = 27$ state. Based on the dependences shown in Fig. 22, the authors drew the following conclusions about the photoionisation process:

— for extremely low fluences, the photoionisation yield is independent of the pulse length and increases linearly with luminosity;

— as the luminosity is increased, the growth of the yield slows down relative to the linear dependence;

— the slowing down is related to the intensity rather than fluence: it appears earlier and proceeds faster for short pulses compared with longer ones;

— for the maximum fluence employed, the short-pulse photoionisation yield is roughly half the corresponding value for a long pulse long pulse.

It should be noted that the data of Fig. 15 are obtained at the fluence $H = 7$ J cm^{-2} (marked by an arrow in Fig. 22), which corresponds to the point at which the intensity-related slowing down of the photoionisation yield starts to be seen. This suggests that the pulse-length dependence of the yield as presented in Ref. 15 is determined not only by the condition $t_l < t_{an}$, as argued in Section 7.1, but also by the intensity.

However, there may be an alternative explanation to account for the sum total of the data of Ref. [72], one based on the assumption of the interference stabilisation of the

$27d$ barium state. As already mentioned (see Section 5), theory predicts interference stabilisation for laser fields $F > F_c = \omega^{5/3}$. From the data of Ref. [72], the experimental results in Figs 15 and 22 are readily found to be obtained in the intensity range from $I_{min} = 3 \times 10^{12}$ W cm^{-2} (at $t_l = 2.7$ ps) to $I_{max} = 3 \times 10^{13}$ W cm^{-2} (at $t_l = 0.25$ ps). In the former case, the field strength is $F \cong F_c = \omega^{5/3}$ and, in the latter, $F \cong 3F_c$. Clearly, the slower growth of the yield with increasing luminosity and its pulse-length dependence are consistent with the basic views on the intensity dependence of the interference stabilisation effect.

It should be kept in mind, however, that one cannot ignore the l splitting of the initial $27d$ state in the radiation field. On the one hand, the splitting may change the value of the critical stabilisation field and, on the other, it must suppress the photoionisation yield from the entire manifold of states with different l.

Note that the alternative explanation we offer for the experimental results of Ref. [72] requires that photoionisation suppression at $t_l < t_{an}$ should also be taken into account.

The above example shows that because of its very nature (mixing of many bound states via the continuum), interference stabilisation presents a challenge for anyone trying to obtain conclusive experimental results.

In summary, there is at present no unequivocal experimental confirmation of the existence of interference stabilisation, but some experiments are to some extent consistent with this hypothesis.

7.4 Stabilisation in photoionisation from an isolated excited state

In the case of an isolated excited state which does not mix with other states when under a strong external field, adiabatic stabilisation may occur. As mentioned above, this takes a relatively higher radiation intensity than, for example, in the case of interference stabilisation. The critical field $F_c = \omega^2 n^2$ is determined by the condition that the free-electron oscillation amplitude start to exceed the size of the Kepler orbit, $a = F/\omega^2 = n^2$.

This value is about n^2 times the critical field for the interference stabilisation as given by Eqn (52), $F_c = \omega^{5/3}$. The adiabatic stabilisation condition for an excited atom might at first sight seem unrealistic because at a significantly lower field a quasicontinuum of ionisation-broadened levels will appear. This conclusion, however, is true only for excited states of very large n value (Rydberg spectrum having a regular structure with a level separation of $\Delta E = n^{-3}$), for $l \sim 1$ [ensuring the validity of the quasiclassical matrix element leading to Eqn (52)], and under the assumption that the initial state does not split (see the discussion at the end of Section 5). However, this conclusion will be incorrect if the following two conditions are fulfilled. First, if the states used are those with small n, in the spectral region where $\Delta E > n^{-3}$. Second, if the initial state has the maximum possible l: for large l the bound–free matrix element is much lower than the quasiclassical estimate used in deriving Eqn (52). The fulfillment of these two conditions may reduce significantly the field strength at which a continuum of adjacent levels appears. The experiment described in Refs [85–86] demonstrates this point.

The aim of the experiment was to observe the adiabatic stabilisation of photoionisation from an isolated excited atomic state.

In order to have the initial excited state isolated, and to avoid l splitting and continuum-assisted state mixing, the state to be excited was taken to be a circular $m = l = n - 1 = 4$ one, and the photoionisation radiation with a spectral width of less than the level separation was used.

The relatively large value of l secured a relatively small photoionisation probability and thus reduced the role of the 'death valley' in the ionising pulse rise, so that the majority of the atoms remained in their excited states until the instant the pulse peak had been reached.

The excited circular state was produced by multiphoton excitation of the atom from its ground state with circularly polarised radiation [77]. By absorbing five photons of the radiation, a neon atom was excited from the ground state $2p^8$ ($m = -1$) to $5g$, $m = l = n - 1 = 4$, with binding energy $E_{5g} = 0.55$ eV and Kepler period of $t_{5g} = 0.6$ ps.

There was a delay of 20 ps introduced between the excitation and ionisation pulses, during which circular atomic states were in a static magnetic field of 1 T. By the use of the Larmor precession occurring in the field (a quarter cycle for 20 ps), the axis of rotational symmetry of the circular states was forced into the polarisation plane of the photoionising radiation. Calculations show—and experiment confirms—that this orientation is optimal for stabilisation.

Photoionisation from the neon $5g$ circular state was achieved by radiation of frequency $\omega = 2$ eV $> E_{5g}$, and pulse length $t_l = 0.1$ ps and $t_l = 1.0$ ps. The exciting and ionising radiations were focused such that the diameter of the focused circle in the former case was much smaller than in the latter. This reduced the inhomogeneity of the spatial distribution of the ionising radiation in the region of ion formation. The photoelectrons were detected and their energies measured. From the photoelectron spectrum given in Ref. [86] it is clearly seen that both the state under study and a number of adjacent states remain discrete, their width being several times less than their spacing. By varying the spectral width of the ionising radiation, the length of the pulse was varied. Pulse lengths of 0.1 and 1.0 ps were used. With a fixed pulse energy this enabled order-of-magnitude intensity changes to be obtained.

The results of the experiment are presented in Fig. 23. It will be seen that the fluence (and intensity) dependences of the photoelectron yield differ qualitatively for the short and long radiation pulses (i. e., for a high and low radiation intensity, respectively). For a long pulse ($t_l = 1.0$ ps) and peak intensity $I = 1.2 \times 10^{13}$ W cm^{-2}, the photoionisation yield increases approximately linearly with the fluence (intensity). For a short pulse ($t_l = 0.1$ ps) and peak intensity $I = 1.2 \times 10^{14}$ W cm^{-2}, it is virtually independent of luminosity (intensity). This is the main piece of evidence for the stabilisation of excited atomic states in this experiment. Another is the radiation intensity value at which the photoionisation yield becomes intensity independent. Experiment gives $I_c = 2 \times 10^{13}$ W cm^{-2}, and calculation $I_c = 5 \times 10^{13}$ W cm^{-2}. The agreement between these two results may be considered to be very good (note that $a = F/\omega^2 = r_{5g}$ in this case). The experimental data of Ref. [86] confirm that the initial state remains isolated; neither splitting nor continuum-assisted mixing occurs. This is seen, for example, from the photoelectron energy spectrum, with a distinct narrow peak for $5g$ photoionisation.

However, the absolute magnitudes of the photoelectron yield for short and long pulses suggest that the radiation

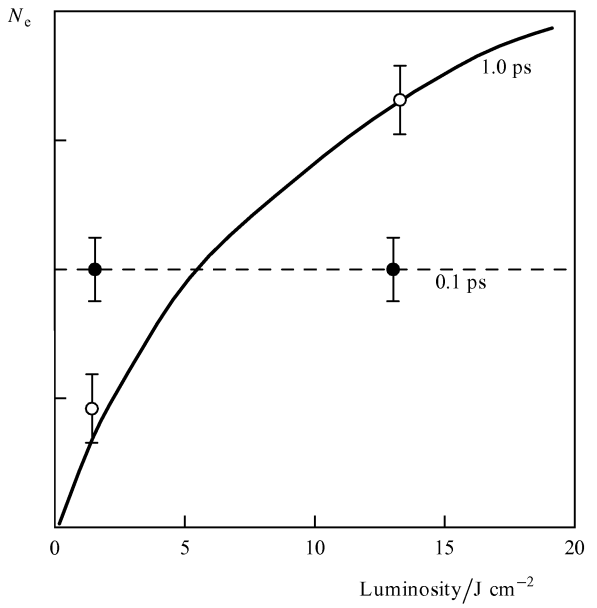

Figure 23. Photoelectron yield from the 5*g* neon state versus fluence for two pulse lengths. Experimental data are taken from Ref. [86].

intensity is not the only contributing factor in this experiment. Changing from fluence to intensity, it is found that the left end of the short-pulse dependence virtually matches the right end of the long-pulse dependence. But the yield amplitudes differ significantly at this point, the short-pulse amplitude being about half the long-pulse value. This discrepancy can be attributed to the suppression of photoionisation at short ($t_l < t_{5g}$) pulse lengths, as discussed in Section 7.1. In fact, for the 5*g* Kepler period, $t_{5g} = 0.6$ ps, the long period obeys the inequality $t_l > t_{5g}$, whereas for the short pulse we have $t_l > t_{5g}$. It is not clear why the authors of Ref. [86] failed to exploit the above-mentioned effect when illustrating good agreement between experimental results and unpublished calculations based on Ref. [43].

As a whole, however, we may summarise by saying that the results of this experiment agree both qualitatively and quantitatively with the theoretical predictions about the conditions for the adiabatic stabilisation of excited atoms.

The global analysis of the experiments on the stabilisation of excited atoms supports the conclusion we have suggested in the introduction to this section — that there are a whole series of experiments consistent with the notion of stabilisation. Of these, however, only one — the neon experiment of Ref. [86] — admits of an unambiguous interpretation. Unfortunately, no other reported experiment is as detailed and comprehensive as this one, which leaves no question unanswered.

Although it is relatively simple and a bit straightforward, there is no reason to question the interpretation given in Ref. [86] of experiments on isolated excited states. It is therefore along these lines that detailed studies on the photoionisation stability of excited atoms under intense laser radiation can be expected.

8. Conclusions

As is traditional, we conclude with a brief outline of the general conclusions and by indicating problems which, although relevant, have been left out of this review.

The most well-founded of our conclusions rests on theory: calculations within different approximations share the property of predicting atomic stabilisation in a super-intense laser radiation field. In a given approach, a certain particular qualitative difference between the quantum 'atom + field' system and the initial atomic structure gives rise to the effect. Reasons for the effect vary. In particular, critical field parameters — for example, the critical field strength — may be numerically different. Theory does not predict a single universal reason for the existence of stabilisation. The reason which is common to all situations is that the atomic structure undergoes qualitative changes as an external laser field with the critical values of its basic parameters is turned on.

Experimental results are still very scarce, especially when compared with the theoretical ones. As of now, the neon experiment of Ref. [86] is the only one to indicate strongly the existence of the effect of adiabatic stabilisation. Further progress in the area is dependent mainly on experimental advances.

As regards the theory, there is only one question which seems to require closer investigation: the competition between photoionisation and induced radiation scattering at the critical field frequency and strength values. Studies along these lines are underway (see Refs [87–92]), but a general picture is still lacking. It is evident, however, that certain scattering features, whether it be Rayleigh- or Raman-type, linear or nonlinear scattering, may have a significant effect on the photoionisation probability and distort the stabilisation picture.

In the case of negative ions, the first thing to note is that there is currently great interest in the problem of photodetachment stabilisation. The central role of the shape of the interaction potential in the stabilisation effect is seen from calculations [67] for various parameters of the long-range potential. Predictions for short-range potentials are contradictory. In a zero-range potential, no stabilisation has been found [17, 20] while it has been found in a finite-range square well [29]. Clearly, further theoretical work will be needed to make reliable predictions, with the specific negative ion structure taken into account. We should also note that a negative ion is a very promising target experimentally, both because of the relatively low affinity of the attached electron and because bound electronic states are few.

Finally, associated with the existence or absence of stabilisation is the question of the limiting value of the AC-Stark level shift. This is, in other words, the question of the possibility of a so-called Stark atom [1, 93–95], when the quantum 'atom + field' system is in a state such that the electron binding energy is much larger than the ionisation potential of the initial atom. The problem of limiting energies of the Stark atom is one of the fundamental questions which still remain to be answered with regard to the atom–field interaction.

As for the questions which, although of relevance to the theme, have been left out of this review, the stabilisation of molecules is the most important one. As usual, however, the range of possibilities is much wider in molecules than in

atoms. The reasons for this are familiar: the more complex spectrum of bound states and the possibility of molecular dissociation. By and large, stabilisation in molecules is a separate and intriguing problem.

In conclusion, atomic stabilisation is, in our opinion, the most interesting effect among those involved in the interaction of intense laser radiation with atoms.

Acknowledgements. The authors express their gratitude to M V Fedorov, for many critical comments on the manuscript, and to participants in the Seminar on Multiphoton Processes at the Institute for General Physics of the Russian Academy of Sciences, for many helpful discussions on the subject matter of the review. The financial support of the International Science Foundation is gratefully acknowledged.

References

1. Delone N B, Krainov V P *Multiphoton Processes in Atoms* (Heidelberg: Springer, 1994)
2. Gavrila M, in *Atoms in Intense Laser Fields* (Ed. M Gavrila) (New York: Academic Press, 1992) p. 435
3. Delone N B, Krainov V P *Usp. Fiz. Nauk* **161** 141 (1991) [*Sov. Phys. Usp.* **34** 1047 (1991)]
4. Burnett K, Reed V, Knight P *J. Phys. B* **26** 561 (1993)
5. Eberly J H, Kulander K *Science* **262** 1229 (1993)
6. Keldysh L V *Zh. Eksp. Teor. Fiz.* **47** 1945 (1964) [*Sov. Phys. JETP* **20** 1307 (1965)]
7. Faisal F H M *J. Phys. B* **6** (L89) (1973)
8. Reiss H R *Phys. Rev. A* **22** 1786 (1980)
9. Reiss H R *Progr. Quantum Electron* **16** 1 (1992)
10. Reiss H R, Krainov V P *Phys. Rev. A* **50** R910 (1994)
11. Neto H, Davidovich L *Phys. Rev. Lett.* **53** 2238 (1984)
12. Geltman S *J. Phys. B* **27** 257 (1994)
13. Geltman S, Teague M *J. Phys.* **7** L22 (1974)
14. Mittleman M H *Introduction to the Theory of Laser–Atom Interactions* (New York: Plenum, 1993)
15. Delone N B, Krainov V P *Atoms in Strong Light Fields* (Heidelberg: Springer, 1985)
16. Reiss H R *Phys. Rev. A* **46** 391 (1992)
17. Grozdanov T, Krstic P *Phys. Lett. A* **149** 144 (1990)
18. Reiss H R *Phys. Rev.* (1995) (to be published)
19. Mohideen U et al. *Phys. Rev. Lett.* **71** 509 (1993)
20. Krainov V P, Preobrazhenskii M A *Zh. Eksp. Teor. Fiz.* **103** 1143 (1993) [*J. Exper. Theor. Phys.* **76** 559 (1993)]
21. Manakov N L, Rapoport L P *Zh. Eksp. Teor. Fiz.* **69** 842 (1975) [*Sov. Phys. JETP* **42** 430 (1975)]
22. Dorr M, Potvliege R M, Shakeshaft R *Phys. Rev. Lett.* **64** 2003 (1990)
23. Pont M, Proulx D, Shakeshaft R *Phys. Rev. A* **44** 4486 (1991)
24. Karule E *Adv. Atom. Mol. Phys.* **26** 265 (1990)
25. Kulander K C, Schafer K J, Krause J L *Phys. Rev. Lett.* **66** 2601 (1991)
26. Grobe R, Eberly J H *Phys. Rev. A* **47** R1605 (1993)
27. Eberly J H *Acta Phys. Pol. A* **86** 151 (1994)
28. Geltman S *Phys. Rev. A* **45** 5293 (1992)
29. Volkova E A, Popov A M *Zh. Eksp. Teor. Fiz.* **105** 1559 (1994) [*J. Exp. Theor. Phys.* **78** 840 (1994)]
30. Henneberger W C *Phys. Rev. Lett.* **21** 838 (1968)
31. Pont M, Gavrila M *Phys. Rev. Lett.* **65** 2362 (1990)
32. Pont M, Gavrila M *Phys. Lett. A* **123** 469 (1987)
33. Pont M *Phys. Rev. A* **40** 5659 (1990)
34. Su Q, Eberly J H, Javanainen J *Phys. Rev. Lett.* **64** 861 (1990)
35. Reed V C, Burnett K *Phys. Rev. A* **42** 3152 (1990)
36. Pont M, Walet N R, Gavrila M, MacCurdy C *Phys. Rev. Lett.* **61** 939 (1988)
37. Su Q, Eberly J H *Phys. Rev. A* **43** 2474 (1991)
38. Potvliege R, Shakeshaft R, in *Atoms in Intense Laser Fields* (Ed. M Gavrila) (New York: Academic Press, 1992) p. 373
39. Faisal F H M, Dimon L *Acta Phys. Pol. A* **86** 201 (1994)
40. Breuer H P, Dietz K, Holthaus M *Phys. Lett. A* **165** 341 (1992)
41. You L, Mostowski J, Cooper J *Phys. Rev. A* **45** 3203 (1992)
42. Vos R J, Gavrila M *Phys. Rev. Lett.* **68** 170 (1992)
43. Potvliege R M, Smith P H G *Phys. Rev. A* **48** R46 (1993)
44. Scrinzi A, Elander N, Piraux B *Phys. Rev. A* **48** R2527 (1993)
45. Volkova E A, Popov A M, Smirnova O V *Zh. Eksp. Teor. Fiz.* **106** 1360 (1994) [*J. Exp. Theor. Phys.* **79** 736 (1994)]
46. Movsesian A M, Fedorov M V *Zh. Eksp. Teor. Fiz.* **95** 47 (1989) [*Sov. Phys. JETP* **68** 27 (1989)]
47. Burnett K, Knight P L, Piraux B R, Reed V C *Phys. Rev. Lett.* **66** 301 (1991)
48. Grobe R, Fedorov M V *Phys. Rev. Lett.* **68** 2592 (1992)
49. Dubrovskii Yu V, Ivanov M Yu, Fedorov M V *Laser Phys.* **2** 288 (1992)
50. Fedorov M V *Comments Atom. Mol. Phys.* **27** 203 (1992)
51. Fedorov M V *Elektron v Sil'nom Svetovom Pole* (Electron in a Strong Light Field) (Moscow: Nauka, 1991)
52. Gontier Y, Rachman N K, Trahin M *Europhys. Lett.* **5** 595 (1988)
53. Delone N B, Fedorov M V *Progr. Quantum Electron.* **13** 267 (1989)
54. Krainov V P, Smirnov B M *Izluchatel'nye Protsessy v Atomnoi Fizike* (Radiative Processes in Atomic Physics) (Moscow: Vysshaya Shkola, 1983), p. 169 [Krainov V P, Smirnov B M, Reiss H *Radiative Processes in Atomic Physics* (New York: Wiley, in press)]
55. Fedorov M V, Movsesian A M *J. Opt. Soc. Am.* **B6** 928 1504 (1989)
56. Delone N B, Goreslavsky S P, Krainov V P *J. Phys. B* **16** 2369 (1983); **22** 2941 (1989)
57. Fedorov M V *Acta Phys. Pol. A* **86** 235 (1994)
58. Goreslavskii S P, Delone N B, Krainov V P *Zh. Eksp. Teor. Fiz.* **82** 1789 (1982) [*Sov. Phys. JETP* **55** 1032 (1982)]
59. Fedorov M V *J. Phys. B* **27** 4145 (1994)
60. Ivanov M Yu *Phys. Rev. A* **49** 1165 (1994)
61. Parzynski R, Wojcik A, Schmidt J *Phys. Rev. A* **50** 3285 (1994)
62. Wocik A, Parzynski R *Phys. Rev. A* **50** 2475 (1994)
63. Nefedov A L *Zh. Eksp. Teor. Fiz.* **100** 803 (1991) [*Sov. Phys. JETP* **73** 444 (1991)]
64. Jensen R V, Sundaram B *Phys. Rev. A* **47** 1415 (1993)
65. Casati G, Guarneri I, Mantica G *Phys. Rev. A* **50** 5018 (1994)
66. Grochmalicki J, Lewenstein M, Rzazewski K *Phys. Rev. Lett.* **66** 1038 (1991)
67. Menis T, Taieb R, Veniard V, Maquet A *J. Phys. B* **25** L263 (1992)
68. Benvenuto F, Casati G, Shepelyansky D L *Phys. Rev. A* **45** R7670 (1992)
69. Benvenuto F, Casati G, Shepelyansky D L *Phys. Rev. A* **47** R786 (1993)
70. Delone N B, Krainov V P, Shepelyanskii D L *Usp. Fiz. Nauk* **140** 355 (1983) [*Sov. Phys. Usp.* **26** 551 (1983)]
71. Rzazewski K, Lewenstein M, Salieres P *Phys. Rev. A* **49** 1196 (1994)
72. Hoogenraad J, Vrijen R, Noordam L *Phys. Rev. A* **50** 4133 (1994)
73. Ritus V *Zh. Eksp. Teor. Fiz.* **51** 1544 (1966) [*Sov. Phys. JETP* **24** 1041 (1967)]
74. Manakov N L, Ovsiannikov V D, Rapoport L P *Phys. Rev.* **141** 321 (1986)
75. Noordam L et al. *Phys. Rev. A* **40** 6999 (1989)
76. Jones R, Bucksbaum P *Phys. Rev. Lett.* **67** 3215 (1991)
77. de Boer M, Noordam L, Muller H *Phys. Rev. A* **47** R45 (1993)
78. Delande D, Goy J *Europhys. Lett.* **5** 303 (1988); Here J, Gross M, Goy J *Phys. Rev. Lett.* **61** 2938 (1988)
79. Randall A, Hulet G, Kleppner D *Phys. Rev. Lett.* **51** 1430 (1983); Nussenzveig P, Bernardot F, Brune M et al. *Phys. Rev. A* **48** 3991 (1993)
80. Delone N B, Krainov V P *Laser Phys.* **2** 654 (1992)
81. Delone N B, Kiyan I Yu, Krainov V P *Laser Phys.* **3** 312 (1993)
82. de Boer M, Muller H *Phys. Rev. Lett.* **68** 2747 (1992)

83. Jones R, Schumacher D, Bucksbaum P *Phys. Rev. A* **47** R49 (1993)
84. Noordam L et al. *Phys. Rev. Lett.* **68** 1496 (1992)
85. de Boer M, Hoogenraad J, Vrijen B et al. *Phys. Rev. Lett.* **71** 3263 (1993)
86. de Boer M, Hoogenraad J, Vrijen B et al. *Phys. Rev. A* **50** 4085 (1994)
87. Kulander K C, Schafer K J, Krause J L, in *Multiphoton Processes, Proc. of the 5th International Conference, Paris, France, September 24–28, 1990* (Eds G Mainfray, P Agostini) (Paris: CEA, 1991)
88. Burnett K, Reed V C, Cooper J, Knight P L *Phys. Rev. A* **45** 3347 (1992)
89. Reed V C, Burnett K, Knight P L *Phys. Rev. A* **47** R34 (1993)
90. Mittleman M H *Phys. Rev. A* **46** 4209 (1992)
91. Nefedov A L *Laser Phys.* **3** 661 (1993)
92. Potvliege R M, Smith P H, in *Proc. of the NAT O Adv. Research Workshop on Super-Intense Laser–Atom Physics* (SILAP 3) (Ed. B Piraux) (New York: Plenum, 1994)
93. Delone N B, Ivanov M Ya, Nefedov A L, in *Multiphoton Processes. Proc. of the 5th International Conference, Paris, France, 24–28 September, 1990* (Eds G Mainfray, P Agostini) (Paris: CEA, 1991) p. 7
94. Delone N B, in *Multiphoton Processes* (Eds D Evans, S L Chin) (Singapore: World Scientific, 1994) p. 461
95. Delone N B *Laser Phys.* (1995) (to be published)